DOI: 10.1002/((please add manuscript number))
Article type: Progress Report

3D Interfacing Between Soft Electronic Tools and Complex Biological Tissues

Hegeng Li, Hongzhen Liu, Mingze Sun, YongAn Huang and Lizhi Xu**

H. Li, H. Liu, M. Sun, Prof. L. Xu
Department of Mechanical Engineering
The University of Hong Kong
Hong Kong SAR 999077, China
E-mail: L. Xu, xulizhi@hku.hk

H. Li, Prof. Y. A. Huang
State Key Laboratory of Digital Manufacturing Equipment and Technology
Huazhong University of Science and Technology
Wuhan 430074, China
E-mail: Y. A. Huang, yahuang@hust.edu.cn

Keywords: soft electronics, 3D bioelectronics, biomedical devices, biointerfaces, physiological sensing and stimulation

Abstract:

Recent developments in soft functional materials have created opportunities for building bioelectronic devices with tissue-like mechanical properties. Their integration with the human body could enable advanced sensing and stimulation for medical diagnosis and therapies. However, most of the available soft electronics are constructed as planar sheets, which are difficult to interface with the target organs and tissues that have complex 3D structures. Here, we highlight the recent approaches to building 3D interfaces between soft electronic tools and complex biological organs and tissues. Examples involve mesh devices for conformal contact, imaging-guided fabrication of organ-specific electronics, miniaturized probes for neuro-interfaces, instrumented scaffold for tissue engineering, and many other soft 3D systems. They represent diverse routes for reconciling the interfacial mismatches between electronic tools and biological tissues. The remaining challenges include device scaling to approach the complexity of target organs, biological data acquisition and processing, 3D manufacturing techniques, etc., providing a range of opportunities for scientific research and technological innovation.

1. Introduction

The past decade witnessed a rapid development of soft electronic devices with mechanical characteristics approaching those of soft biological tissues.[1] Unlike traditional electronics based on rigid semiconductor chips and circuit boards, these soft devices possess Young's moduli at the levels ranging from kPa to GPa, with a reversible elongation of up to 1000%. They could minimize the mechanical mismatch at the biotic-abiotic interface, enabling a variety of sensors and stimulators for continuous health monitoring, interventional therapies, fundamental physiological investigation, tissue engineering, and many other applications.

Essential to these tissue-like electronic devices are the constituent soft materials and their fabrication techniques. Polymers and composites provide intrinsic tolerance to strain.[2] Inorganic nanostructures impart high electronic properties without compromising the deformability at the device level.[3] Methods adapted from microelectronic manufacturing provide available routes for patterning and integration of these materials into hybrid systems. However, as exemplified by wafer-based thin-film deposition, photolithography and etching, the typical fabrication processes are designed primarily for planar devices. Consequently, electronics involving soft constituents mostly remain with two-dimensional (2D) features, with a typical form resembling a plastic sheet. These devices are capable of integration over a small area on the human body with low topographic variation. For instance, small electronic patches are usually laminated on the forearm for the measurement of temperature, pulse wave, bioelectricity and/or blood oxygenation, providing medical utilities.[4]

However, the human body involves many important organs with structural complexity far beyond the intrinsic features of electronic sheets. For instance, the brain involves billions of neurons interconnected in the highly folded cerebral cortex, which cannot be accurately mapped with only a planar device. Moreover, the neuronal activities take place not only on the surface but also in the deep layers of the brain, creating difficulties for brain-machine interfacing. The heart involves four muscular chambers with highly dynamic structures. The electro-mechanical

coupling in a complex 3D fashion makes cardiac electronic interfaces challenging. Although the stiffness and elasticity of soft electronics could match those of the natural tissues, their physical embodiment as 2D sheets may hinder advanced integration on the brain, the heart and other sophisticated 3D organs.

In this Progress Report, we highlight some of the recent strategies on transforming soft electronic tools for building 3D biointerfaces. We start with a brief overview on soft electronic materials. The materials toolbox enables various deformation mechanisms which is essential for 3D architecture of soft devices. The discussion expands on a range of 3D electronic systems for biomedical applications. For devices integrated on the contoured organ surfaces, mesh structures and those inspired by kirigami are useful for creating conformal contact. When guided by 3D imaging and modeling of the target organs, devices could be fabricated with specific features matching those in the natural physiology. For interpenetrating neuro-interfaces, device miniaturization is essential for the management of foreign body responses and for probing bioelectricity at the single-neuron level. Furthermore, electronics-embedded cell culture could enable advanced platform for biological research and tissue engineering technology. The examples discussed in the following sections represent diverse routes for building 3D interfaces between soft electronics and biological tissues, suggesting many exciting opportunities for biomedical research.

2. The toolbox of soft electronic materials

The materials approach to soft electronics involves a wide range of inorganic and organic components. As exemplified by single crystalline silicon (Si), inorganic electronic materials possess outstanding electronic properties with mature fabrication techniques. However, due to their intrinsic rigidity and brittleness, their utilization in soft electronics would require additional structural design that accommodates deformation at the device level. Here, nanostructures involving nanoparticle (NP) assembly, nanomembranes (NMs) and nanowires

(NWs) are particularly useful for this purpose. On the other hand, recently emerged polymeric electronic materials could be intrinsically strain-tolerant. They could serve as many key components for devices that undergo mechanical deformation. Furthermore, composites incorporating multiple materials could provide additional options for building soft functional devices. Many of these materials are discussed in detail in other review articles.[2,5,6] Here we highlight some of the latest examples with an emphasis on their mechanical characteristics, which is essential for building 3D biointerfaces.

2.1 Inorganic nanomaterials

Inorganic NMs are extensively used for soft electronics due to their favorable bending characteristics.[7] It is noted that the flexural rigidity of a membrane is proportional to the third power of its thickness. Reducing the thickness from ~1mm to ~10 nm could lead to a reduction in flexural rigidity by 15 orders of magnitude, transforming rigid semiconductor wafers into flexible NMs. Furthermore, NM structures could help to minimize the strain upon bending and the energy release rate associated with delamination from substrates, which prevent mechanical failure of electronic devices. Inorganic NMs can be pattered into a network of ribbons or serpentine traces, imparting modes for in-plane stretching and/or out-of-plane buckling. For instance, Si NMs can be harvested from silicon-on-insulator (SOI) wafers and transfer-printed onto pre-stretched soft elastomer substrates (**Figure 1a**).[8] Upon release of the pre-strain, ribbons of Si NMs could spontaneously assemble into 3D structures due to compressive buckling. Importantly, the strain in the single crystalline Si can be maintained within 1% during the reconfiguration, which is below the threshold of mechanical cracking. 3D architecture involving waves,[9] island-bridges,[10] serpentines,[11] helices,[8] and many other complex structures can be made with various inorganic NMs with excellent electronic properties.[3] They not only accommodate the large macroscopic deformation without compromising electronic functions, but also provide physical interfaces with organs and tissues involving 3D topography.

Utilization of graphene and other 2D nanomaterials in soft electronics also takes advantage of the favorable behaviors of NMs. Their atomic-level thickness imparts outstanding flexibility along with optical transparency. Although the intrinsic stretchability of graphene is around 6%,[12] incorporating a pattern of slits could greatly enhance its tolerance to tension. For instance, graphene bonded to an elastomer substrate could retain good conductance even with 30% of tensile strain.[13,14] In these structures, micro-cracks formed at the initial stage of stretching could accommodate the subsequent tension without causing disintegration of the conduction pathway. In another configuration, patterns inspired by paper-cutting art, or referred to as kirigami, could enable excellent deformability in a well-controlled manner. When parallel and alternating cuts are patterned into a freestanding graphene sheet, a reversible stretchability of up to 240% could be achieved (**Figure 1b**).[15] The deformation scheme and strain distribution with kirigami could be modeled with established theories in continuum mechanics, providing useful design guidelines. In addition, graphene layers assembled in other modes, including those resembling ripples[16] or fish scales,[17] are also explored for building soft electronics. Other 2D nanomaterials including molybdenum disulfide (MoS_2) and hexagonal boron nitride (hBN) were also explored for building soft bioelectronics.[18,19]

One-dimensional (1D) nanostructures, as exemplified by Si NWs, carbon nanotubes (CNTs) and metallic NWs, are popular candidates for building soft electronic sensors.[20] Their nanoscale diameters (~1-50 nm) provide structural flexibility in a similar fashion to those of NMs.[21] In addition to the geometric scaling, intrinsic effects associated with the surfaces and defects in NWs also contribute to their high deformability.[22] Bending experiments on Si NWs showed a high fracture strength (~18 GPa) approaching the theoretical strength of ~20 GPa, as compared with typical values of ~1.5 GPa for bulk samples.[23,24] In-situ tensile tests in a scanning electron microscope (SEM) revealed that Si NWs can withstand 10% of cyclic tensile strains without fracture (**Figure 1c**), which is far beyond the ultimate tensile strain of bulk Si (~1%).[25] For applications in biosensing, the high surface-to-volume ratios of NWs afford

excellent sensitivity to chemical species adsorbed on their surfaces. Furthermore, the dimensions of 1D nanomaterials are comparable with some of the subcellular structures, enabling advanced probes for cellular physiology. Biomedical applications related to these features of 1D nanostructures will be discussed in further sections.

Assembly of inorganic NPs could also enable electronic devices with high deformability. For instance, gold (Au) NPs with a diameter of ~10 nm possess high mobility when dispersed in polyurethane (PU) matrix. Upon mechanical stretching, these NPs can self-organize into conductive chains guided by the deformation of the soft PU (**Figure 1d**).[26] Based on this phenomenon, highly stretchable conductors are made possible with a reversible stretchability of over 100%. In addition, semiconductor NPs, or referred to as quantum dots, are also useful for soft electronics. They are typically constructed as flexible optoelectronic components, serving as the light source or display for bio-integrated systems.[27]

2.2 Polymeric and composite materials

Electro-active polymers have been widely used in soft electronics. The intrinsic deformability of organic polymers arises from the folding and reconfiguration of their macromolecular chains. Polymers involving π-conjugated backbones often exhibit electrical conductivity due to the delocalization of electrons. Tuning of their electronic properties could be achieved with intrinsic molecular design and/or extrinsic doping approaches.[1,28] Typical conducting polymers involve poly(3,4-ethylenedioxythiophene):poly(styrene sulfonate) (PEDOT:PSS), polypyrole (PPy) and polyaniline (PANI). Poly(3-hexylthiophene) (P3HT) and diketopyrrolopyrrole-based (DPP-based) polymers represent some of the semiconducting polymers. Unlike the inorganic microelectronic materials relying on high-temperature and/or high-vacuum processes, many polymeric electronic materials can be prepared with simple, solution-based methods, suggesting possibilities for large scale production with relatively low cost.[29] However, a trade-off exists between the electronic performance of conducting/semiconducting polymers and their mechanical deformability, partly due to the

rigidity and crystalline order of conjugated networks.[30,31] Adding nonionic, fluorinated surfactants into PEDOT:PSS would increase its ductility from 5% to 40%, but with the cost of a reduction of conductivity by a few orders of magnitude.[32] Other approaches based on block copolymers or side chains would usually lead to similar phenomena.[33,34] Recent strategies exploit careful molecular designs to enhance the chain dynamics of conducting polymers with minimal impact on their electronic properties. For instance, PEDOT:PSS added with some ionic compounds could retain a conductivity of 4100 S/cm under 100% tensile strain, as compared to 3100 S/cm for un-stretched samples.[35] DPP-based polymers inserted with non-conjugated, hydrogen-bond-forming moieties could reconfigure under tensile strains without interrupting effective charge transport (**Figure 2a and b**).[36] Their reformable hydrogen bonding would also allow healing of microscopic defects. Blending semiconducting poly(2,5-bis(2-octyldodecyl)-3,6-di(thiophen-2-yl)diketopyrrolo[3,4-c]pyrrole-1,4-dione-alt-thieno[3,2-b]thiophen) (DPPT-TT) with polystyrene-block-poly(ethylene-ran-butylene)-block-polystyrene (SEBS) elastomer would lead to nanoconfinement effects associated with phase separation (**Figure 2c**).[37] The aggregated DPPT-TT forms percolating nanofibril network, providing stable electronic characteristics even under 100% of elongation applied to the elastomeric composites. In addition, embedding P3HT nanofibers into elastomer matrices would also enable stretchable polymeric semiconductors.[38] These and other organic electronic materials are available for integration in arrays of soft sensors or transistors,[39] providing utilities for bioelectronic interfaces.

Composites involving inorganic conductors dispersed in elastomeric matrices represent another useful route for creating soft electronics.[2,40] Inorganic fillers such as CNTs,[41] metallic NWs[42] or NPs[43] could form percolating network for effective charge transport. Soft matrices involving polydimethylsiloxane (PDMS),[44] polyurethane (PU)[26], poly(styrene-butadiene-styrene) (SBS)[45] or other elastomers could withstand large deformation without structural disintegration. The design of composites could benefit from the large library of existing

materials with available processing methods. Recent research demonstrated printable elastic conductors based on silver (Ag) NPs formed in-situ during the fabrication steps (**Figure 2d and e**).[46] These Ag NPs with diameters of ~10 nm are derived from low-cost, micrometer-sized Ag flakes dispersed in fluorinated elastomers. Their formation could be controlled with tuning of surfactants and heating conditions. This soft conductor could retain a conductivity of ~935 S/cm under 400% elongation, as compared with ~6168 S/cm for un-stretched state. 1D nanostructures could form 3D percolated networks more easily than particles with low aspect ratio. While the typical percolation threshold for spherical particles is ~20%,[26] fillings based on CNT or Ag NW could form percolated networks even with a low volume fraction of ~1%.[47] Furthermore, percolated networks of 1D or 2D nanostructures possess a lower sensitivity to macroscopic deformation as compared with network of particles with low aspect ratio.[43,45] This feature indicates selection rules for strain sensing components or strain-invariant interconnects for soft electronics.

Room-temperature liquid metals gain attention as constituents for soft electronic composites. Eutectic alloys based on gallium-indium (EGaIn) or gallium-indium-tin (Galinstan) are popular candidates due to their low vapor pressure and biocompatibility.[48] These Ga-based alloys can form an oxide layer on their surface upon contact with air, providing mechanical stability for patterned structures.[49] Liquid metals are highly reconfigurable. Galinstan droplets dispersed in PDMS (**Figure 2f**) can form patterns of conductive traces upon selective physical compression.[50] Self-healing devices could also benefit from the fluidity of liquid metals.[51] Formation of electronic sensors or actuators usually exploits elastomer matrix for the packaging of liquid metal structures, providing required structural support and elasticity. These devices could be stretched by over 700% without mechanical failure, limited only by the elasticity of polymeric matrix.[52]

Although hydrogels are traditionally used as electro-passive biomaterials, recent research has exploited its utilities as soft bioelectronic components.[53,54] Their electrical conductivity

could be realized by incorporating ions[55] or network of conducting polymers[56] or nanocarbons[57] to their highly porous structures. The advantages of hydrogel-based electronics involve their intrinsic similarity to soft biological tissues. Their low stiffness, high water content and dynamic mechanical behavior could help to minimize adverse physiological responses upon integration with the living body.[58] Prevention of dehydration of hydrogels could be achieved with selective encapsulation with silicone elastomers (**Figure 2g**) or other dense materials.[59]

3. Bioelectronics integrated on 3D organ surfaces

As exemplified by the brain and the heart, human organs involve complex 3D surfaces. Most of these surfaces are non-developable, which exhibit non-zero Gaussian curvatures and cannot be flattened onto a plane without distortion. At the meanwhile, mapping of a planar device to these non-developable surfaces would require anisotropic and non-uniform deformation of the original planar features. Although mathematical guidelines involving differential geometry of soft bioelectronics remain elusive, many engineering designs have led to devices that can accommodate the required deformation. In most of the cases, reducing modulus of the constituent material and thickness of the structure could facilitate 3D deformation with lowered strain energy. Designs involving stretchable mesh and/or kirigami could further minimize the energetic costs for the conformation to organ surfaces. When guided by 3D imaging and printing techniques, devices can be manufactured with specific features matching those of the natural organs. The following discussion highlights some of the recent designs for conformal integration with 3D organ surfaces.

3.1 Mesh devices and structures inspired by kirigami

Mesh structures could afford conformal integration on contoured surfaces. A research on brain-laminated electrodes provides useful mechanical insights to organ-integrated mesh devices.[60] It is noted that contact between a planar-fabricated device and an organ surface is determined by an energetic competition between interfacial adhesion and elastic strain.

Therefore, conformation to a curved surface is possible only if the strain energy from the deformation of the planar features is smaller than the adhesion energy. A simplified model involves wrapping of a device with a bending stiffness of *EI*, modulus of *E*, thickness of *h*, width of *b* and length of *2L* onto a cilinder with a radius of *R* (**Figure 3a**). For a wrapped state that is energetically favorable,

$$\gamma \geq \gamma_c = \frac{EI}{2R^2 b} = \frac{Eh^3}{24R^2} \quad (1)$$

where γ is the adhesion energy per unit area. With a given mode of interfacial adhesion, minimizing the thickness of the device (*h*) and the elastic moduli (*E*) of the constituent materials is essential for conformal wrapping (**Figure 3b**). Furthermore, for the integration on non-developable surfaces, mesh designs could reduce the energetic costs and the membrane strains as compared with continuous films (**Figure 3c**). A theoretical model involves a comparison between a circular strip and a circular sheet to be wrapped onto a spherical surface, indicating the mechanical advantages of mesh designs. In an optimized configuration, a mesh of 30 metallic electrodes with a thickness of ~2.5 μm could integrate with the sophisticated contours of animal cortex, driven merely by capillary forces. They enable mapping of neuronal activities with high spatial resolution and data fidelity. A more recent work demonstrated an array of electrodes integrated on the retina of living animals.[61] This mesh device could conform to the concaved surface of retina and retain a stable contact for over 14 days in awake mice (**Figure 4a**). It enables chronic recording of electrophysiology at single-neuron levels, providing powerful means for the study of neural circuitry. In addition to the designs based on square lattices, meshes involving hexagonal patterns are also considered for conformal bioelectronics.[62,63] In these devices, the hexagonal network could provide some degree of stretchability even with straight and non-wavy structural elements.

Incorporating serpentine patterns in mesh designs could further enhance their conformability to organ surfaces. In addition to their low effective stiffness, these spring-like

patterns could accommodate large in-plane elongation without causing detrimental strains to the constituent materials.[64] Their deformability is further enhanced with modes for out-of-plane buckling and non-homogeneous strain distribution upon mechanical loading.[11] Fractal designs involving hierarchical and self-similar patterns could increase areal filling of the serpentines without compromising high structural deformability.[65] Indeed, the mechanical behaviors of serpentine-based meshes could be modeled with established theories in continuum mechanics, allowing for optimized designs for various applications.[66] For instance, a metallic, filamentary serpentine network supported by soft elastomer membrane could exhibit an effective modulus of ~150 kPa, which is similar to the intrinsic modulus of the human skin.[67,68] Electronics based on this design could be laminated onto the skin in a mechanically imperceptible manner. As predicted by theoretical modeling, the energy release rate for delamination diminishes as the thickness of these soft membranes drops to micrometer-levels. Furthermore, filamentary serpentine meshes could be directly printed onto the skin without soft elastomer backing (**Figure 4b**).[65,69] Such devices could conform to the microscale contour of the skin, providing mechanically stable and low-impedance interfaces for sensing and stimulation. In a recent demonstration, large electrode arrays were fabricated on eight-inch wafers and integrated over the full scalp of human subjects (**Figure 4b**).[70] This system could serve as a brain-machine interface for prosthetic control and cognitive monitoring. In addition to epidermal electronic systems, serpentine meshes could also enable conformal devices for internal organs. For instance, a multifunctional electronic mesh could be integrated on the epicardium driven by capillary forces.[71] However, the weak interfacial interaction in this setting might not be ideal for fully implanted systems that undergo prolonged use. Additional organ-specific designs would be necessary, which will be discussed in the next section.

Engineering structures inspired by paper-cutting art, or referred to as kirigami, have attracted wide attention recently. A most simple configuration of kirigami involves parallel and alternating cuts introduced into a solid film (**Figure 4c**).[72] These cuts could transform an

originally un-stretchable film into highly reconfigurable membrane, with deformation mechanisms similar to those for serpentine meshes. They also impart anisotropic mechanical behaviors in a well-controlled manner. The free combination of available materials and cutting patterns affords almost limitless designs for engineering applications.[73,74] An advantage of kirigami is that it provides high areal coverage without compromising structural deformability. Integration of large-area kirigami to dynamic and curved surfaces is facilitated with multiple mechanisms, including shear-lag effect, partial debonding and inhomogeneous deformation of the substrate.[75] In a recent research, an array of metallic thin-film electrodes was fabricated on a kirigami-patterned parylene sheet.[76] This device exhibits an effective modulus of ~23 kPa and a reversible elongation of ~470%. It is capable of conformal integration on the cortex or epicardium for physiological sensing and stimulation (Figure 4c).

Nanoscale mesh structures are recently explored for building bioelectronic interfaces. For instance, polyvinyl alcohol (PVA) nanofibers with a diameter of 300-500 nm could be generated by electrospinning. These water-dissolvable nanofibers serve as a template for the creation of vacuum-deposited Au nanomeshes, which could be laminated on the fingertip.[77] Upon dissolution of PVA, the layer of Au nanomeshes spontaneously conforms to the microscale contour of the skin (**Figure 4d**), serving as bioelectrodes and/or strain sensors. Compared to traditional electronic skin-patches, these lightweight and "breathable" nanomeshes allow vapor and moisture to escape, leading to minimal degree of discomfort or risk of inflammation. Although these nanomesh electrodes could accommodate some strains, they are prone to fracture when subject to elongation over ~20% or mechanical rubbing. Application for long-term use may require additional designs for improved structural robustness. On the other hand, nanomeshes could couple with mesoscale structures such as serpentines or kirigami. The multiscale mesh designs could enable further enhancement of 3D conformability and fine tuning of the device mechanics.[78]

3.2 Approaches to organ-specific electronics

Typical soft electronics are constructed in a "one-size-fits-all" fashion. However, the lack of custom designs might hinder their practical applications on specific organs. For instance, a generic serpentine mesh could cover a small area of epicardium with capillary forces.[71] However, it is difficult to integrate over the full surface of the heart that undergo dynamic deformation. In addition, its structural fragility and weak interfacial adhesion do not afford long-term use under complex mechanical loading and immersion in biofluids. Addressing these challenges would require attention to organ-specific designs. A recent work exploits 3D imaging and 3D printing methods for the exact matching between soft electronics and cardiac structures (**Figure 5a**).[79] In this scheme, a proportionally scaled model of the real heart serves as a 3D template for creating custom devices. Although planar-fabricated serpentine meshes were involved for the electronic components, the overall geometry and mechanical characteristics of the device were determined by a soft elastomer membrane casted against the 3D-printed model. After removal from the model, this electronics-embedded 3D membrane could be wrapped around the entire epicardium for robust bioelectronic interface. With careful mechanical designs, the elastic forces from the membrane afford stable contact during cardiac cycles. On the other hand, the exerted pressure is sufficiently small and do not interfere with the natural motion of the cardiac structures. These instrumented membranes enable large-area mapping of electrical activation, temperature, strain and pH with high spatiotemporal resolution (**Figure 5b**). They could further allow optical stimulation and delivery of precision electrotherapy to the heart in a feedback-controlled manner.[80] To access the internal surfaces of organs, similar designs could be applied to instrumented balloon catheters. Their reconfiguration affords both minimally invasive intervention and expansion to match the geometry of complex cavities.[81]

The combination of 3D imaging and 3D printing techniques could enable conformal electronics directly fabricated on curved surfaces. Advanced inks with tunable viscosity allow for direct writing of functional materials in 3D.[82,83] Electrohydrodynamic (EHD) lithography

could generate nanoscale features on contours.[84,85] When combined with 3D imaging modalities, these and other techniques for direct writing could enable custom fabrication of organ-conformal electronics. For instance, an integrated close-loop system could fabricate electronic circuits on free-moving human hands (**Figure 5c**).[86] In this setup, the 3D geometry and the motion of the hand are tracked with an optical scanner and computer vision. Printing of electrical connects and placing of miniaturized chips can be controlled with real-time inputs of geometrical information of the moving hand. Furthermore, for soft tissues undergoing complex expansion and contraction, machine learning could be applied to obtain accurate surface information via dynamic point-cloud analysis.[87] These automated systems enable rapid and custom fabrication of conformal devices, suggesting routes to advanced wearable technologies.

4. Interpenetrating 3D biointerfaces

Interrogating brain activities represents one of the major motivations for developing advanced bioelectronics. However, the cerebral neural network involves only on the surface of the cortex but also the deep layers of the brain. Surface mounted devices are not able to characterize the full 3D picture involving both low-frequency local field potential (LFP) and high-frequency action potential of neurons.[88] Therefore, invasive probes are often required. After implantation, these probes occupy the original space of functional tissues, causing forced rearrangement of the neurons and glial cells. Furthermore, they disrupt the blood-brain-barrier (BBB) and form device-tissue interfaces that are prone to chemical degradation, relative motion and unwanted injury/immune responses, which severely compromise the device functionality.[89,90] To mitigate these impacts, minimizing the feature size and the bending stiffness of brain probes is crucial. Chemical modifications to the devices could also help to modulate tissue responses.[91] In addition, multiplexed devices could help to resolve the spatiotemporal patterns of LFP and cellular activities, and to deliver targeted stimulation. Recent efforts were devoted to addressing these issues, leading to neural probes with increasing

levels of functionality and compatibility with the natural tissues. These devices could enable interpenetrating neuro-electronic interfaces, complementing functional magnetic resonance imaging (fMRI), calcium or voltage indicators, surface-mounted electrodes and other techniques for advanced neuroscience.

4.1. Miniaturized probes with integrated bioelectronics

Since its first demonstration in 1957, microwire electrodes have been extensively adopted for probing neural activities.[92] In addition to their minimal invasiveness, it is believed that electrodes with diameters below 10 μm are desirable for resolving unitary spikes from individual neurons. A recent work demonstrated advanced composite microwires for chronic recording of brain activities on living rats (**Figure 6a**).[93] These devices involve 7-μm-diameter carbon fibers coated with ~800 nm of parylene-N via chemical vapor deposition (CVD). A ~200-nm-thick layer of poly(ethylene glycol) methacrylate (PEGMA) was polymerized on the surface of the fibers to prevent non-specific adsorption of plasma proteins. Nanotextured PEDOT:PSS was electrochemically deposited on the tip of the carbon fiber, serving as low-impedance electrochemical interface. These flexible probes afford stable in-vivo recording of single-neuron activities for over five weeks upon implantation. As compared with millimeter-scale shaft electrodes, these composite microwires significantly reduce the levels of acute injury and subsequent foreign body responses, leading to chronically stable bioelectronic interfaces. Microwire electrodes can be bundled up to allow multichannel recordings.[94,95] However, high density mapping is difficult to achieve with typical microwires partly due to the limitations in their fabrication techniques. Furthermore, charge injection capacity and electrochemical corrosion might restrict their application in chronic stimulation.[96]

Manufacturing technologies for Si-based microelectronics enabled multiplexed probes for high-density neural recording. A Michigan-type device involves a narrow shank with electrodes distributed along the length of the probe.[97] A Utah-type device exploits a bulk-micromachined array of Si needles, with the tips serving as the recording sites.[98] Although they are not as

deformable as recently developed soft devices, these classic tools have enabled extensive studies on neuroscience and neuro-prosthetics.[99,100] A recent system, referred to as Neuropixels, involves 960 electrodes integrated on a Michigan-type probe, suitable for chronic in-vivo measurement of brain activities (**Figure 6c**).[101] These high-density electrodes are driven by complementary metal-oxide-semiconductor (CMOS) components fabricated on the shank, with the voltage signals filtered, amplified and digitized on the base of the device. This 10-milimeter-long probe could interface with multiple structures of the brain along the depth of penetration, generating distinguishable signals from over 700 individual neurons of an awake mouse. In addition, Michigan-type probes could be tessellated in the transverse directions to generate a hybrid array (**Figure 6b**).[102] Such array integrates 1024 electrodes for neural recording in a 3D fashion. Although Si-based probes are useful, the increasing number of electrodes might lead to invasiveness to the brain tissues, high electrochemical impedance or burden for thermal management.[103–105] The rigid Si structures can be replaced with soft polymers for a tissue-compliant interface,[106,107] but the tradeoff mentioned above may still exist.

Physiological research involving optogenetics could benefit from multifunctional neural probes. In addition to electrical sensing and stimulation, these probes deliver optical pulses to the genetically modified targets, enabling precise control of neuronal activities.[105] For instance, a thermally drawn multi-material fiber could integrate six electrodes, one optical waveguide and two microfluidic channels.[108] It allows delivery of viral vectors carrying opsin genes while providing collocated neural recordings and optical stimulation. This multifunctional probe enables an integrated system for optogenetic experiments on the animal brains, with only one-step implantation. Another type of probe exploits microscale light emitting diodes (μ-LEDs) directly implanted into the brain (**Figure 6d**).[109] These μ-LEDs are supported by soft polymeric substrates that can be injected into the brain structures. Multimodal sensors for temperature, bioelectricity and strain, as well as microfluidic channels, can be fabricated on the

optoelectronic probe for physiological monitoring and drug delivery.[105,110–112] In addition, this design could transform into cuff probes for integration with peripheral nerves.[113] These probes connect to miniaturized wireless modules, allowing for full operation on free-moving animals.

4.2 Injectable mesh electronics

Unlike the traditional neural probes, mesh devices could interrogate a volume of brain structures without excessive disruption of the natural tissues. Their flexibility and porosity enable adaptive and interpenetrating tissue-electronics interfaces, leading to lower degree of foreign body responses and relative motion as compared with traditional probes. Recent efforts were devoted to injectable mesh electronics for chronically stable brain-machine interfaces.[114,115] A typical configuration involves thin-film metallic electrodes insulated with soft polymers, and microfabricated into an open network. The mesh device could fit in a glass capillary with a diameter of ~100 μm (**Figure 7a**).[115] Upon syringe-injection into the brain, the mesh unfolds spontaneously and integrate with the 3D structures of neural tissues (**Figure 7b**). Connection to external hardware could be accomplished after the injection, as the base of the mesh remains outside of the brain tissues.[116–118] An alternative design exploits surface tension of water for folding an input/output(I/O)-connected mesh into a micro-cylinder. After freezing, this free-standing cylinder could be directly inserted into the brain without using a syringe, avoiding the separate process for I/O connection.[119] Injection of the mesh electronics could be controlled by stereotaxic instrument, allowing for targeting to specific brain structures.[61,120] Although the mesh devices are compliant to the neural tissues, managing the acute injuries from the insertion might require extensive attention.

A recent research demonstrated mesh electronics with the size and mechanics approaching those of natural neurons.[121] This device, referred to as neuron-like electronics (NeuE), involves 16 electrodes constructed in an open network. The feature size of the device (1-20 μm) is similar to those of the soma and neurite of typical pyramidal neuron (**Figure 7c**). The ultrathin polymer structures (~1 μm) afford a low bending stiffness (~0.087 nN/m) comparable to those of axons.

After implantation, the NeuE forms interpenetrating interfaces with the neurons, with less than 0.3% of the volume occupied by the device (**Figure 7d**). In contrast to traditional probes, the NeuE does not lead to an obvious depletion of neurons or proliferation of astrocytes in the vicinity, indicating a minimal level of injury or foreign body response. These implanted electrodes maintain fixed positions relative to the surrounding tissue, affording stable recording of the same set of individual neurons for over 90 days on living mice. The NeuE could characterize 3D patterns of the neural signals with micrometer-scale resolution, providing useful information for functional mapping of the brain. Furthermore, as indicated by both electrical recordings and histology, the NeuE could promote migration of newborn neurons into the open network. This phenomenon suggests further possibilities of modulating cell behaviors in vivo.

5. 3D soft electronics for advanced cell and tissue culture

The previous discussion was mainly focused on 3D soft electronics designed for in-vivo applications. On the other hand, in-vitro studies involving cell and tissue culture are indispensable for biomedical research. These experiments provide a simplified and well-controlled environment for fundamental investigation of biological processes and development of therapeutic strategies. Electronic devices compatible with cell and tissue culture could enable real-time monitoring and/or targeted stimulation, providing an advanced toolbox for physiological research. This section will highlight some of the recent devices for creating 3D adaptive interfaces with isolated cells and tissues. The emerging strategies for soft electronics have enabled systems with functionalities far beyond their traditional counterparts. Examples involve scalable probes for intracellular recordings and instrumented scaffolds for synthetic tissues, among many other applications.

5.1. Emerging tools for intracellular recordings

Probing physiological signals from the intracellular space represent an area of major interest. For instance, the full electrophysiological repertoire of a neuron involves subthreshold

synaptic potentials, membrane oscillations and action potentials, which is difficult to capture without accessing both sides of the cell membrane.[122] The LFP measured by typical extracellular electrodes misses significant details of the cellular activities, with the peaks representing only partial components from the action potential. Traditional intracellular recordings rely on patch-clamp experiments.[123] Although useful, this method requires sophisticated manipulation and it is difficult to scale up for long-term measurement or simultaneous recording on multiple cells. Recent development in 3D nanodevices has led to many advanced systems with capabilities beyond those of patch-clamp setup. For instance, electrodes constructed as vertical nanopillars could spontaneously form a tight interface with the cell membrane (**Figure 8a and b**).[124] Their access to the intracellular space could be achieved by membrane fusion,[125,126] endocytosis,[127] electroporation,[128] optoacoustic effects[129] or other techniques. Many of these methods lead to reversible changes in the cell membrane with minimal impact on the natural cellular physiology. The subsequent intracellular measurement could capture fine details of the electrophysiological processes, which is in a steep contrast with recordings from the extracellular space (**Figure 8c**).[130] In addition, localized stimulation to individual cells is possible with these culture-embedded nanopillar electrodes, enabling studies of electro-mechanical coupling of cardiomyocytes (**Figure 8c**) or many other experiments.

Si-based device technologies could facilitate the creation of advanced 3D cell-electronics interfaces. Nanowires or nanopillars can be fabricated with techniques ranging from top-down approaches involving reactive ion etching (RIE)[124] and focused ion beam (FIB) milling,[126,128] to bottom-up methods involving vapor-liquid-solid (VLS) growth[125] and electroplating.[131] These fabrication methods afford diverse routes for building 3D electronic tools embedded in the cell culture. Furthermore, Si-based integrated circuits could enable high-density arrays of intracellular electrodes for measuring hundreds of cells.[129,130] Such platforms allow for network-level mapping, providing key capabilities for both fundamental research and

pharmacological screening. In addition to the direct electrical interfaces, Si-based devices could interact with cells in many other domains. For instance, bending of flexible Si NWs could enable measurement of cellular mechanics.[132] Photovoltaic effects in coaxial p-type/intrinsic/n-type Si NWs could be utilized for stimulating neurons via electrochemical reactions.[133]

Although many of the intracellular tools mentioned above are constructed on rigid platforms, their fundamental concepts provide inspirations for creating 3D probes with soft mechanical behaviors. For instance, Si NWs could be bent into a U-shape and deterministically assembled on soft polymeric substrates.[134] After fabrication into field-effect transistors (FETs), these NW devices could be released form the rigid handling wafer, forming freestanding probes (**Figure 8d**). The high surface-to-volume ratio of NWs and their operation as FETs afford excellent sensitivity to voltage signals. Interactions with the cell membrane can be controlled with the tip geometry and sensor size, along with the chemical modifications to NWs. These freestanding probes enable active tracking of cells and recording of up to 100 mV of intracellular action potentials. Furthermore, these NW-FET sensors can be constructed in a scalable manner. Arrays of these probes can be configured for modes of multiplexed recording (**Figure 8e**).[135] They provide advanced means for studying dynamics of single cells, cell networks and functional tissues.

5.2. Electronic scaffold for synthetic tissues

Engineering functional tissues in vitro is essential for regenerative medicine, disease modeling, pharmaceutical biotechnology and many other applications. Traditional methods for tissue engineering rely on electro-passive biomaterials.[136] Their limited capability in spatiotemporal sensing and stimulation creates difficulties for precise control of tissue formation. Recently emerged electronic meshes are showing their promises for addressing this challenge. Their advantages for tissue engineering involve: (i) structural flexibility to match the mechanics and topography of soft tissues, (ii) capabilities in large-area mapping and stimulation,

and (iii) high porosity to support tissue assembly and nutrient transport. For instance, a porous electronic mesh involving 64 FET sensors could be embedded in a cardiac tissue culture.[137] Construction of 3D interface is achieved with manual folding and stacking of the electronic mesh. This scaffold enables real-time measurement of propagation of action potential at the tissue level, providing an advanced alternative to the traditional fluorescent experiment.[138] Furthermore, nanofibers could be incorporated into the scaffold to mimic the extracellular matrix, providing a robust interface between cells and electronic devices (**Figure 9a and b**).[139,140] Nanofiber-based scaffold is adaptive to the motion of cardiomyocytes, allowing for stable recording for over 96 hours.[140] In addition, electronic scaffolds could be constructed with multiple functions (**Figure 9a**).[139] Integrated components for electrical sensing, stimulation, cell attachment, drug release and other utilities enable controlled interactions with the tissue in many domains.

Soft electronic scaffolds could enable dynamic 3D tissues via self-folding. Mechanisms involving extrinsic forces or intrinsic stresses allow for a variety of reconfigurable 3D structures.[74,141] For instance, controlled buckling of NMs could lead to a complex 3D architecture at micro-/meso-scale (**Figure 1a**). Electronics fabricated with such architecture could be used to guide the formation of cardiac or nervous tissues.[142,143] An advantage of this 3D platform is that it allows structural reconfiguration via applied strains. Tissues could be cultured in one configuration and transform into another via active structural modulation. This feature will facilitate studies on the dynamics of electrogenic tissue network. Another example involves electronics-embedded organoids (**Figure 9c**).[144] In this scheme, the process of organogenesis is coupled with the adaptation of a stretchable electronic mesh. The cell-cell attraction forces lead to self-folding of a composite tissue-electronics sheet. After 3 to 20 days of co-culturing, a stem-cells-derived cardiac organoid could form with an integrated electronic network. The embedded sensors enable continuous monitoring of electrophysiological signals during the process of organogenesis, providing powerful means for physiological research.

Recent advances in 3D bio-printing allow for custom fabrication of tissue-electronics complex. For instance, a flexible antenna could be co-printed with chondrocyte-seeded hydrogels, forming an "bionic ear".[145] Tactile sensors could be 3D fabricated within prostate tissue models.[146] Integrating impedance-based chemical sensors in cartilage tissues leads to an "hybrid nose".[147] Although promising, these 3D-printed prototypes have yet to demonstrate sophisticated bioelectronic interactions. Further development on functional inks and high-resolution bioprinting might help to address this limitation.

6. Summary and outlook

The examples discussed above represent diverse strategies for building 3D interfaces between soft electronics and complex biological organs and tissues. These designs provide advanced means for obtaining important physiological information and for delivering targeted stimulation. With these 3D electronic interfaces, a range of experiments for biological research or therapeutic innovation become possible, otherwise difficult to accomplish with traditional tools. Development in soft materials and their fabrication techniques will continue to expand the design toolbox for advanced 3D bioelectronics, creating opportunities for biomedical applications.

Some of the key challenges may require further attention. First, the functionality of existing soft electronics has yet to match the complexity of natural tissues. For instance, the brain involves billions of neurons interconnected in sophisticated networks, which cannot be fully deciphered with devices involving only ~100 electrodes. This limitation is partly related to the fabrication capabilities available to typical biomedical research labs. Fortunately, the modern microelectronics industry has established processes for large-scale integration of high-density microdevices. Collaboration with industrial platforms would facilitate the creation of systems with number/density of the sensors far beyond those of the existing prototypes.[148] Incorporating high-density semiconductor electronics for signal amplification and/or multiplexing would be essential for these sophisticated devices.[101,130] In addition, solutions for

energy and wireless commnucation for these bio-integrated systems might require further attention.[149,150]

The second challenge involves data interpretation for the emerging modes of measurement. Established analytic methods were mostly designed for the traditional biomedical tools, which might not be ideal for the data generated from 3D mapping with advanced soft bioelectronics. In addition, as the number of sensors scales up, the volume of information could exceed the capacity of traditional analytic protocols. The emerging techniques in artificial intelligence might help to address this challenge. For instance, algorithms for pattern recognition could analyze recordings from 548 sensors integrated on a tactile glove.[151] With a brief process of machine learning, it becomes possible to recognize the signature of human grasp and to perceive the weights and dimensions of various objects.

The third challenge is related to standardized fabrication. Most of the existing 3D soft bioelectronics involves manual assembly of the devices. Although their functionalities are well-demonstrated, developing commercial products would require scalable methods for manufacturing. Recently emerged techniques for 3D fabrication suggest a couple of useful routes.[152] For instance, pneumatically inflated elastomeric balloons could be used as stamps for transferring microdevices on curved surfaces.[153] This method may enable automated manufacturing of organ-conformal electronics. In addition, 3D printing techniques could couple with dynamic morphing of the printed structures.[154] The hybrid method, referred to as 4D printing, involves mathematical analyses for the precise assembly of 3D structures with non-uniform Gaussian curvatures. This approach may help to fabricate adaptive soft devices in a scalable manner. These and other manufacturing techniques could facilitate the development of commercial soft bioelectronics, providing further capabilities for standardized experiment and clinical translation.

Acknowledgement:

L.X. acknowledge support from Research Grant Council (Grant No. 27210019 and 17200320). Y. A. Huang acknowledge support from the National Natural Science Foundation of China (Grant No. 51925503 and 51635007).

Conflict of Interest:

The authors declare no conflict of interest.

Received: ((will be filled in by the editorial staff))
Revised: ((will be filled in by the editorial staff))
Published online: ((will be filled in by the editorial staff))

Reference

[1] T. R. Ray, J. Choi, A. J. Bandodkar, S. Krishnan, P. Gutruf, L. Tian, R. Ghaffari, J. A. Rogers, *Chem. Rev.* **2019**, *119*, 5461.
[2] N. Matsuhisa, X. Chen, Z. Bao, T. Someya, *Chem. Soc. Rev.* **2019**, *48*, 2946.
[3] Z. Xue, H. Song, J. A. Rogers, Y. Zhang, Y. Huang, *Adv. Mater.* **2020**, *32*, 1902254.
[4] Y. Ma, Y. Zhang, S. Cai, Z. Han, X. Liu, F. Wang, Y. Cao, Z. Wang, H. Li, Y. Chen, X. Feng, *Adv. Mater.* **2020**, *32*, 1902062.
[5] S. Choi, S. I. Han, D. Kim, T. Hyeon, D. H. Kim, *Chem. Soc. Rev.* **2019**, *48*, 1566.
[6] C. Wang, C. Wang, Z. Huang, S. Xu, *Adv. Mater.* **2018**, *30*, 1801368.
[7] J. A. Rogers, M. G. Lagally, R. G. Nuzzo, *Nature* **2011**, *477*, 45.
[8] S. Xu, Z. Yan, K. I. Jang, W. Huang, H. Fu, J. Kim, Z. Wei, M. Flavin, J. McCracken, R. Wang, A. Badea, Y. Liu, D. Xiao, G. Zhou, J. Lee, H. U. Chung, H. Cheng, W. Ren, A. Banks, X. Li, U. Paik, R. G. Nuzzo, Y. Huang, Y. Zhang, J. A. Rogers, *Science.* **2015**, *347*, 154.
[9] Y. Sun, W. M. Choi, H. Jiang, Y. Y. Huang, J. A. Rogers, *Nat. Nanotechnol.* **2006**, *1*, 201.
[10] H. C. Ko, M. P. Stoykovich, J. Song, V. Malyarchuk, W. M. Choi, C.-J. Yu, J. B. Geddes III, J. Xiao, S. Wang, Y. Huang, J. A. Rogers, *Nature* **2008**, *454*, 748.
[11] D. H. Kim, J. Song, M. C. Won, H. S. Kim, R. H. Kim, Z. Liu, Y. Y. Huang, K. C. Hwang, Y. W. Zhang, J. A. Rogers, *Proc. Natl. Acad. Sci. U. S. A.* **2008**, *105*, 18675.
[12] K. Cao, S. Feng, Y. Han, L. Gao, T. Hue Ly, Z. Xu, Y. Lu, *Nat. Commun.* **2020**, *11*, 284.
[13] K. S. Kim, Y. Zhao, H. Jang, S. Y. Lee, J. M. Kim, K. S. Kim, J. H. Ahn, P. Kim, J. Y. Choi, B. H. Hong, *Nature* **2009**, *457*, 706.
[14] N. Liu, A. Chortos, T. Lei, L. Jin, T. R. Kim, W. G. Bae, C. Zhu, S. Wang, R. Pfattner, X. Chen, R. Sinclair, Z. Bao, *Sci. Adv.* **2017**, *3*, e1700159.
[15] M. K. Blees, A. W. Barnard, P. A. Rose, S. P. Roberts, K. L. McGill, P. Y. Huang, A. R. Ruyack, J. W. Kevek, B. Kobrin, D. A. Muller, P. L. McEuen, *Nature* **2015**, *524*, 204.
[16] Y. Wang, R. Yang, Z. Shi, L. Zhang, D. Shi, E. Wang, G. Zhang, *ACS Nano* **2011**, *5*, 3645.
[17] Q. Liu, J. Chen, Y. Li, G. Shi, *ACS Nano* **2016**, *10*, 7901.
[18] M. Park, Y. J. Park, X. Chen, Y. K. Park, M. S. Kim, J. H. Ahn, *Adv. Mater.* **2016**, *28*, 2556.

[19] L. Wu, J. Shi, Z. Zhou, J. Yan, A. Wang, C. Bian, J. Ma, R. Ma, H. Liu, J. Chen, Y. Huang, W. Zhou, L. Bao, M. Ouyang, S. T. Pantelides, H. J. Gao, *Nano Res.* **2020**, *13*, 1127.
[20] Z. Liu, J. Xu, D. Chen, G. Shen, *Chem. Soc. Rev.* **2015**, *44*, 161.
[21] D. M. Tang, C. L. Ren, M. S. Wang, X. Wei, N. Kawamoto, C. Liu, Y. Bando, M. Mitome, N. Fukata, D. Golberg, *Nano Lett.* **2012**, *12*, 1898.
[22] Q. Liu, L. Wang, S. Shen, *Comput. Mater. Sci.* **2015**, *101*, 267.
[23] R. F. Cook, *J. Mater. Sci.* **2006**, *41*, 841.
[24] G. Stan, S. Krylyuk, A. V. Davydov, I. Levin, R. F. Cook, *Nano Lett.* **2012**, *12*, 2599.
[25] H. Zhang, J. Tersoff, S. Xu, H. Chen, Q. Zhang, K. Zhang, Y. Yang, C.-S. Lee, K.-N. Tu, J. Li, Y. Lu, *Sci. Adv.* **2016**, *2*, e1501382.
[26] Y. Kim, J. Zhu, B. Yeom, M. Di Prima, X. Su, J. G. Kim, S. J. Yoo, C. Uher, N. A. Kotov, *Nature* **2013**, *500*, 59.
[27] M. K. Choi, J. Yang, T. Hyeon, D.-H. Kim, *npj Flex. Electron.* **2018**, *2*, 10.
[28] S. Wang, J. Y. Oh, J. Xu, H. Tran, Z. Bao, *Acc. Chem. Res.* **2018**, *51*, 1033.
[29] T. Sekitani, R. Someya, *Adv. Mater.* **2010**, *22*, 2228.
[30] C. Müller, S. Goffri, D. W. Breiby, J. W. Andreasen, H. D. Chanzy, R. A. J. Janssen, M. M. Nielsen, C. P. Radano, H. Sirringhaus, P. Smith, N. Stingelin-Stutzmann, *Adv. Funct. Mater.* **2007**, *17*, 2674.
[31] B. O'Connor, E. P. Chan, C. Chan, B. R. Conrad, L. J. Richter, R. J. Kline, M. Heeney, I. McCulloch, C. L. Soles, D. M. DeLongchamp, *ACS Nano* **2010**, *4*, 7538.
[32] S. Savagatrup, E. Chan, S. M. Renteria-Garcia, A. D. Printz, A. V. Zaretski, T. F. O'Connor, D. Rodriquez, E. Valle, D. J. Lipomi, *Adv. Funct. Mater.* **2015**, *25*, 427.
[33] L. V. Kayser, M. D. Russell, D. Rodriquez, S. N. Abuhamdieh, C. Dhong, S. Khan, A. N. Stein, J. Ramírez, D. J. Lipomi, *Chem. Mater.* **2018**, *30*, 4459.
[34] G. J. N. Wang, L. Shaw, J. Xu, T. Kurosawa, B. C. Schroeder, J. Y. Oh, S. J. Benight, Z. Bao, *Adv. Funct. Mater.* **2016**, *26*, 7254.
[35] Y. Wang, C. Zhu, R. Pfattner, H. Yan, L. Jin, S. Chen, F. Molina-Lopez, F. Lissel, J. Liu, N. I. Rabiah, Z. Chen, J. W. Chung, C. Linder, M. F. Toney, B. Murmann, Z. Bao, *Sci. Adv.* **2017**, *3*, e1602076.
[36] J. Y. Oh, S. Rondeau-Gagné, Y.-C. Chiu, A. Chortos, F. Lissel, G.-J. N. Wang, B. C. Schroeder, T. Kurosawa, J. Lopez, T. Katsumata, J. Xu, C. Zhu, X. Gu, W.-G. Bae, Y. Kim, L. Jin, J. W. Chung, J. B.-H. Tok, Z. Bao, *Nature* **2016**, *539*, 411.
[37] J. Xu, S. Wang, G.-J. N. Wang, C. Zhu, S. Luo, L. Jin, X. Gu, S. Chen, V. R. Feig, J. W. F. To, S. Rondeau-Gagné, J. Park, B. C. Schroeder, C. Lu, J. Y. Oh, Y. Wang, Y.-H. Kim, H. Yan, R. Sinclair, D. Zhou, G. Xue, B. Murmann, C. Linder, W. Cai, J. B.-H. Tok, J. W. Chung, Z. Bao, *Science.* **2017**, *355*, 59.
[38] E. Song, B. Kang, H. H. Choi, D. H. Sin, H. Lee, W. H. Lee, K. Cho, *Adv. Electron. Mater.* **2016**, *2*, 1500250.
[39] S. Wang, J. Xu, W. Wang, G. J. N. Wang, R. Rastak, F. Molina-Lopez, J. W. Chung, S. Niu, V. R. Feig, J. Lopez, T. Lei, S. K. Kwon, Y. Kim, A. M. Foudeh, A. Ehrlich, A. Gasperini, Y. Yun, B. Murmann, J. B. H. Tok, Z. Bao, *Nature* **2018**, *555*, 83.
[40] D. C. Kim, H. J. Shim, W. Lee, J. H. Koo, D.-H. Kim, *Adv. Mater.* **2020**, *32*, 1902743.
[41] M. K. Shin, J. Oh, M. Lima, M. E. Kozlov, S. J. Kim, R. H. Baughman, *Adv. Mater.* **2010**, *22*, 2663.
[42] P. Song, H. Qin, H.-L. Gao, H.-P. Cong, S.-H. Yu, *Nat. Commun.* **2018**, *9*, 2786.
[43] M. Park, J. Im, M. Shin, Y. Min, J. Park, H. Cho, S. Park, M. Shim, S. Jeon, D. Chung, J. Bae, J. Park, U. Jeong, K. Kim, *Nat. Nanotechnol.* **2012**, *7*, 803.
[44] F. Xu, Y. Zhu, *Adv. Mater.* **2012**, *24*, 5117.

[45] S. Choi, S. I. Han, D. Jung, H. J. Hwang, C. Lim, S. Bae, O. K. Park, C. M. Tschabrunn, M. Lee, S. Y. Bae, J. W. Yu, J. H. Ryu, S. W. Lee, K. Park, P. M. Kang, W. B. Lee, R. Nezafat, T. Hyeon, D. H. Kim, *Nat. Nanotechnol.* **2018**, *13*, 1048.
[46] N. Matsuhisa, D. Inoue, P. Zalar, H. Jin, Y. Matsuba, A. Itoh, T. Yokota, D. Hashizume, T. Someya, *Nat. Mater.* **2017**, *16*, 834.
[47] J. Li, P. C. Ma, W. S. Chow, C. K. To, B. Z. Tang, J. Kim, *Adv. Funct. Mater.* **2007**, *17*, 3207.
[48] Y. Lu, Q. Hu, Y. Lin, D. B. Pacardo, C. Wang, W. Sun, F. S. Ligler, M. D. Dickey, Z. Gu, *Nat. Commun.* **2015**, *6*, 10066.
[49] C. Ladd, J.-H. So, J. Muth, M. D. Dickey, *Adv. Mater.* **2013**, *25*, 5081.
[50] A. Fassler, C. Majidi, *Adv. Mater.* **2015**, *27*, 1928.
[51] E. J. Markvicka, M. D. Bartlett, X. Huang, C. Majidi, *Nat. Mater.* **2018**, *17*, 618.
[52] S. Zhu, J. H. So, R. Mays, S. Desai, W. R. Barnes, B. Pourdeyhimi, M. D. Dickey, *Adv. Funct. Mater.* **2013**, *23*, 2308.
[53] H. Yuk, B. Lu, X. Zhao, *Chem. Soc. Rev.* **2019**, *48*, 1642.
[54] C. Yang, Z. Suo, *Nat. Rev. Mater.* **2018**, *3*, 125.
[55] C. Keplinger, J. Sun, C. C. Foo, P. Rothemund, G. M. Whitesides, Z. Suo, *Science.* **2013**, *341*, 984.
[56] B. Lu, H. Yuk, S. Lin, N. Jian, K. Qu, J. Xu, X. Zhao, *Nat. Commun.* **2019**, *10*, 1043.
[57] S. R. Shin, S. M. Jung, M. Zalabany, K. Kim, P. Zorlutuna, S. B. Kim, M. Nikkhah, M. Khabiry, M. Azize, J. Kong, K. T. Wan, T. Palacios, M. R. Dokmeci, H. Bae, X. Tang, A. Khademhosseini, *ACS Nano* **2013**, *7*, 2369.
[58] Y. Liu, J. Liu, S. Chen, T. Lei, Y. Kim, S. Niu, H. Wang, X. Wang, A. M. Foudeh, J. B. H. Tok, Z. Bao, *Nat. Biomed. Eng.* **2019**, *3*, 58.
[59] H. Yuk, T. Zhang, G. A. Parada, X. Liu, X. Zhao, *Nat. Commun.* **2016**, *7*, 12028.
[60] D.-H. Kim, J. Viventi, J. J. Amsden, J. Xiao, L. Vigeland, Y.-S. Kim, J. A. Blanco, B. Panilaitis, E. S. Frechette, D. Contreras, D. L. Kaplan, F. G. Omenetto, Y. Huang, K.-C. Hwang, M. R. Zakin, B. Litt, J. A. Rogers, *Nat. Mater.* **2010**, *9*, 511.
[61] G. Hong, T. M. Fu, M. Qiao, R. D. Viveros, X. Yang, T. Zhou, J. M. Lee, H. G. Park, J. R. Sanes, C. M. Lieber, *Science.* **2018**, *360*, 1447.
[62] Y. K. Lee, K.-I. Jang, Y. Ma, A. Koh, H. Chen, H. N. Jung, Y. Kim, J. W. Kwak, L. Wang, Y. Xue, Y. Yang, W. Tian, Y. Jiang, Y. Zhang, X. Feng, Y. Huang, J. A. Rogers, *Adv. Funct. Mater.* **2017**, *27*, 1605476.
[63] M. K. Kim, C. Kantarcigil, B. Kim, R. K. Baruah, S. Maity, Y. Park, K. Kim, S. Lee, J. B. Malandraki, S. Avlani, A. Smith, S. Sen, M. A. Alam, G. Malandraki, C. H. Lee, *Sci. Adv.* **2019**, *5*, eaay3210.
[64] Y. Su, X. Ping, K. J. Yu, J. W. Lee, J. A. Fan, B. Wang, M. Li, R. Li, D. V Harburg, Y. Huang, C. Yu, S. Mao, J. Shim, Q. Yang, P.-Y. Lee, A. Armonas, K.-J. Choi, Y. Yang, U. Paik, T. Chang, T. J. Dawidczyk, Y. Huang, S. Wang, J. A. Rogers, *Adv. Mater.* **2017**, *29*, 1604989.
[65] J. A. Fan, W.-H. Yeo, Y. Su, Y. Hattori, W. Lee, S.-Y. Jung, Y. Zhang, Z. Liu, H. Cheng, L. Falgout, M. Bajema, T. Coleman, D. Gregoire, R. J. Larsen, Y. Huang, J. A. Rogers, *Nat. Commun.* **2014**, *5*, 3266.
[66] N. Lu, S. Yang, *Curr. Opin. Solid State Mater. Sci.* **2015**, *19*, 149.
[67] D. H. Kim, N. Lu, R. Ma, Y. S. Kim, R. H. Kim, S. Wang, J. Wu, S. M. Won, H. Tao, A. Islam, K. J. Yu, T. Il Kim, R. Chowdhury, M. Ying, L. Xu, M. Li, H. J. Chung, H. Keum, M. McCormick, P. Liu, Y. W. Zhang, F. G. Omenetto, Y. Huang, T. Coleman, J. A. Rogers, *Science.* **2011**, *333*, 838.
[68] K.-I. Jang, H. U. Chung, S. Xu, C. H. Lee, H. Luan, J. Jeong, H. Cheng, G.-T. Kim, S. Y. Han, J. W. Lee, J. Kim, M. Cho, F. Miao, Y. Yang, H. N. Jung, M. Flavin, H. Liu, G.

W. Kong, K. J. Yu, S. Il Rhee, J. Chung, B. Kim, J. W. Kwak, M. H. Yun, J. Y. Kim, Y. M. Song, U. Paik, Y. Zhang, Y. Huang, J. A. Rogers, *Nat. Commun.* **2015**, *6*, 6566.
[69] W. H. Yeo, Y. S. Kim, J. Lee, A. Ameen, L. Shi, M. Li, S. Wang, R. Ma, S. H. Jin, Z. Kang, Y. Huang, J. A. Rogers, *Adv. Mater.* **2013**, *25*, 2773.
[70] L. Tian, B. Zimmerman, A. Akhtar, K. J. Yu, M. Moore, J. Wu, R. J. Larsen, J. W. Lee, J. Li, Y. Liu, B. Metzger, S. Qu, X. Guo, K. E. Mathewson, J. A. Fan, J. Cornman, M. Fatina, Z. Xie, Y. Ma, J. Zhang, Y. Zhang, F. Dolcos, M. Fabiani, G. Gratton, T. Bretl, L. J. Hargrove, P. V. Braun, Y. Huang, J. A. Rogers, *Nat. Biomed. Eng.* **2019**, *3*, 194.
[71] D. H. Kim, R. Ghaffari, N. Lu, S. Wang, S. P. Lee, H. Keum, R. D'Angelo, L. Klinker, Y. Su, C. Lu, Y. S. Kim, A. Ameen, Y. Li, Y. Zhang, B. De Graff, Y. Y. Hsu, Z. J. Liu, J. Ruskin, L. Xu, C. Lu, F. G. Omenetto, Y. Huang, M. Mansour, M. J. Slepian, J. A. Rogers, *Proc. Natl. Acad. Sci. U. S. A.* **2012**, *109*, 19910.
[72] T. C. Shyu, P. F. Damasceno, P. M. Dodd, A. Lamoureux, L. Xu, M. Shlian, M. Shtein, S. C. Glotzer, N. A. Kotov, *Nat. Mater.* **2015**, *14*, 785.
[73] Y. Cho, J. H. Shin, A. Costa, T. A. Kim, V. Kunin, J. Li, S. Y. Lee, S. Yang, H. N. Han, I. S. Choi, D. J. Srolovitz, *Proc. Natl. Acad. Sci. U. S. A.* **2014**, *111*, 17390.
[74] L. Xu, T. C. Shyu, N. A. Kotov, *ACS Nano* **2017**, *11*, 7587.
[75] R. Zhao, S. Lin, H. Yuk, X. Zhao, *Soft Matter* **2018**, *14*, 2515.
[76] Y. Morikawa, S. Yamagiwa, H. Sawahata, R. Numano, K. Koida, M. Ishida, T. Kawano, *Adv. Healthc. Mater.* **2018**, *7*, 1701100.
[77] A. Miyamoto, S. Lee, N. F. Cooray, S. Lee, M. Mori, N. Matsuhisa, H. Jin, L. Yoda, T. Yokota, A. Itoh, M. Sekino, H. Kawasaki, T. Ebihara, M. Amagai, T. Someya, *Nat. Nanotechnol.* **2017**, *12*, 907.
[78] S. Huang, Y. Liu, C. F. Guo, Z. Ren, *Adv. Electron. Mater.* **2017**, *3*, 1600534.
[79] L. Xu, S. R. Gutbrod, A. P. Bonifas, Y. Su, M. S. Sulkin, N. Lu, H.-J. Chung, K.-I. Jang, Z. Liu, M. Ying, C. Lu, R. C. Webb, J.-S. Kim, J. I. Laughner, H. Cheng, Y. Liu, A. Ameen, J.-W. Jeong, G.-T. Kim, Y. Huang, I. R. Efimov, J. A. Rogers, *Nat. Commun.* **2014**, *5*, 3329.
[80] L. Xu, S. R. Gutbrod, Y. Ma, A. Petrossians, Y. Liu, R. C. Webb, J. A. Fan, Z. Yang, R. Xu, J. J. Whalen, J. D. Weiland, Y. Huang, I. R. Efimov, J. A. Rogers, *Adv. Mater.* **2015**, *27*, 1731.
[81] D. H. Kim, N. Lu, R. Ghaffari, Y. S. Kim, S. P. Lee, L. Xu, J. Wu, R. H. Kim, J. Song, Z. Liu, J. Viventi, B. De Graff, B. Elolampi, M. Mansour, M. J. Slepian, S. Hwang, J. D. Moss, S. M. Won, Y. Huang, B. Litt, J. A. Rogers, *Nat. Mater.* **2011**, *10*, 316.
[82] J. J. Adams, E. B. Duoss, T. F. Malkowski, M. J. Motala, B. Y. Ahn, R. G. Nuzzo, J. T. Bernhard, J. A. Lewis, *Adv. Mater.* **2011**, *23*, 1335.
[83] A. D. Valentine, T. A. Busbee, J. W. Boley, J. R. Raney, A. Chortos, A. Kotikian, J. D. Berrigan, M. F. Durstock, J. A. Lewis, *Adv. Mater.* **2017**, *29*, 1703817.
[84] Y. Huang, N. Bu, Y. Duan, Y. Pan, H. Liu, Z. Yin, Y. Xiong, *Nanoscale* **2013**, *5*, 12007.
[85] Y. Liu, Y. Huang, *J. Micromechanics Microengineering* **2019**, *29*, 065002.
[86] Z. Zhu, S.-Z. Guo, T. Hirdler, C. Eide, X. Fan, J. Tolar, M. C. McAlpine, *Adv. Mater.* **2018**, *30*, 1707495.
[87] Z. Zhu, H. S. Park, M. C. McAlpine, *Sci. Adv.* **2020**, *6*, eaba5575.
[88] G. Hong, C. M. Lieber, *Nat. Rev. Neurosci.* **2019**, *20*, 330.
[89] T. D. Y. Kozai, A. S. Jaquins-Gerstl, A. L. Vazquez, A. C. Michael, X. T. Cui, *ACS Chem. Neurosci.* **2015**, *6*, 48.
[90] R. Feiner, T. Dvir, *Nat. Rev. Mater.* **2017**, *3*, 17076.
[91] J. A. Goding, A. D. Gilmour, U. A. Aregueta-Robles, E. A. Hasan, R. A. Green, *Adv. Funct. Mater.* **2018**, *28*, 1702969.
[92] D. H. Hubel, *Science.* **1957**, *125*, 549.

[93] T. D. Y. Kozai, N. B. Langhals, P. R. Patel, X. Deng, H. Zhang, K. L. Smith, J. Lahann, N. A. Kotov, D. R. Kipke, *Nat. Mater.* **2012**, *11*, 1065.
[94] J. E. Ferguson, C. Boldt, A. D. Redish, *Sensors Actuators, A Phys.* **2009**, *156*, 388.
[95] A. Obaid, M. E. Hanna, Y. W. Wu, M. Kollo, R. Racz, M. R. Angle, J. Müller, N. Brackbill, W. Wray, F. Franke, E. J. Chichilnisky, A. Hierlemann, J. B. Ding, A. T. Schaefer, N. A. Melosh, *Sci. Adv.* **2020**, *6*, eaay2789.
[96] J. A. Fairfield, *Adv. Funct. Mater.* **2018**, *28*, 1701145.
[97] D. J. Anderson, K. Najafi, S. J. Tanghe, D. A. Evans, K. L. Levy, J. F. Hetke, X. Xue, J. J. Zappia, K. D. Wise, *IEEE Trans. Biomed. Eng.* **1989**, *36*, 693.
[98] P. K. Campbell, K. E. Jones, R. J. Huber, K. W. Horch, R. A. Normann, *IEEE Trans. Biomed. Eng.* **1991**, *38*, 758.
[99] L. R. Hochberg, M. D. Serruya, G. M. Friehs, J. A. Mukand, M. Saleh, A. H. Caplan, A. Branner, D. Chen, R. D. Penn, J. P. Donoghue, *Nature* **2006**, *442*, 164.
[100] E. M. Trautmann, S. D. Stavisky, S. Lahiri, K. C. Ames, M. T. Kaufman, D. J. O'Shea, S. Vyas, X. Sun, S. I. Ryu, S. Ganguli, K. V Shenoy, *Neuron* **2019**, *103*, 292.
[101] J. J. Jun, N. A. Steinmetz, J. H. Siegle, D. J. Denman, M. Bauza, B. Barbarits, A. K. Lee, C. A. Anastassiou, A. Andrei, Ç. Aydin, M. Barbic, T. J. Blanche, V. Bonin, J. Couto, B. Dutta, S. L. Gratiy, D. A. Gutnisky, M. Häusser, B. Karsh, P. Ledochowitsch, C. M. Lopez, C. Mitelut, S. Musa, M. Okun, M. Pachitariu, J. Putzeys, P. D. Rich, C. Rossant, W. L. Sun, K. Svoboda, M. Carandini, K. D. Harris, C. Koch, J. O'Keefe, T. D. Harris, *Nature* **2017**, *551*, 232.
[102] J. E. Chung, H. R. Joo, J. L. Fan, D. F. Liu, A. H. Barnett, S. Chen, C. Geaghan-Breiner, M. P. Karlsson, M. Karlsson, K. Y. Lee, H. Liang, J. F. Magland, J. A. Pebbles, A. C. Tooker, L. F. Greengard, V. M. Tolosa, L. M. Frank, *Neuron* **2019**, *101*, 21.
[103] N. A. Steinmetz, C. Koch, K. D. Harris, M. Carandini, *Curr. Opin. Neurobiol.* **2018**, *50*, 92.
[104] G. Rios, E. V. Lubenov, D. Chi, M. L. Roukes, A. G. Siapas, *Nano Lett.* **2016**, *16*, 6857.
[105] T. Il Kim, J. G. McCall, Y. H. Jung, X. Huang, E. R. Siuda, Y. Li, J. Song, Y. M. Song, H. A. Pao, R. H. Kim, C. Lu, S. D. Lee, I. S. Song, G. Shin, R. Al-Hasani, S. Kim, M. P. Tan, Y. Huang, F. G. Omenetto, J. A. Rogers, M. R. Bruchas, *Science.* **2013**, *340*, 211.
[106] L. Luan, X. Wei, Z. Zhao, J. J. Siegel, O. Potnis, C. A. Tuppen, S. Lin, S. Kazmi, R. A. Fowler, S. Holloway, A. K. Dunn, R. A. Chitwood, C. Xie, *Sci. Adv.* **2017**, *3*, e1601966.
[107] E. Musk, *J Med Internet Res* **2019**, *21*, e16194.
[108] S. Park, Y. Guo, X. Jia, H. K. Choe, B. Grena, J. Kang, J. Park, C. Lu, A. Canales, R. Chen, Y. S. Yim, G. B. Choi, Y. Fink, P. Anikeeva, *Nat. Neurosci.* **2017**, *20*, 612.
[109] J. W. Jeong, J. G. McCall, G. Shin, Y. Zhang, R. Al-Hasani, M. Kim, S. Li, J. Y. Sim, K. I. Jang, Y. Shi, D. Y. Hong, Y. Liu, G. P. Schmitz, L. Xia, Z. He, P. Gamble, W. Z. Ray, Y. Huang, M. R. Bruchas, J. A. Rogers, *Cell* **2015**, *162*, 662.
[110] A. D. Mickle, S. M. Won, K. N. Noh, J. Yoon, K. W. Meacham, Y. Xue, L. A. McIlvried, B. A. Copits, V. K. Samineni, K. E. Crawford, D. H. Kim, P. Srivastava, B. H. Kim, S. Min, Y. Shiuan, Y. Yun, M. A. Payne, J. Zhang, H. Jang, Y. Li, H. H. Lai, Y. Huang, S. Il Park, R. W. Gereau, J. A. Rogers, *Nature* **2019**, *565*, 361.
[111] W. Bai, J. Shin, R. Fu, I. Kandela, D. Lu, X. Ni, Y. Park, Z. Liu, T. Hang, D. Wu, Y. Liu, C. R. Haney, I. Stepien, Q. Yang, J. Zhao, K. R. Nandoliya, H. Zhang, X. Sheng, L. Yin, K. MacRenaris, A. Brikha, F. Aird, M. Pezhouh, J. Hornick, W. Zhou, J. A. Rogers, *Nat. Biomed. Eng.* **2019**, *3*, 644.
[112] H. Shin, Y. Son, U. Chae, J. Kim, N. Choi, H. J. Lee, J. Woo, Y. Cho, S. H. Yang, C. J. Lee, I. J. Cho, *Nat. Commun.* **2019**, *10*, 3777.
[113] Y. Zhang, A. D. Mickle, P. Gutruf, L. A. McIlvried, H. Guo, Y. Wu, J. P. Golden, Y. Xue, J. G. Grajales-Reyes, X. Wang, S. Krishnan, Y. Xie, D. Peng, C. J. Su, F. Zhang, J.

T. Reeder, S. K. Vogt, Y. Huang, J. A. Rogers, R. W. Gereau, *Sci. Adv.* **2019**, *5*, eaaw5296.
[114] T. M. Fu, G. Hong, R. D. Viveros, T. Zhou, C. M. Lieber, *Proc. Natl. Acad. Sci. U. S. A.* **2017**, *114*, E10046.
[115] J. Liu, T.-M. Fu, Z. Cheng, G. Hong, T. Zhou, L. Jin, M. Duvvuri, Z. Jiang, P. Kruskal, C. Xie, Z. Suo, Y. Fang, C. M. Lieber, *Nat. Nanotechnol.* **2015**, *10*, 629.
[116] J. M. Lee, G. Hong, D. Lin, T. G. Schuhmann, A. T. Sullivan, R. D. Viveros, H. G. Park, C. M. Lieber, *Nano Lett.* **2019**, *19*, 5818.
[117] T. M. Fu, G. Hong, T. Zhou, T. G. Schuhmann, R. D. Viveros, C. M. Lieber, *Nat. Methods* **2016**, *13*, 875.
[118] T. G. Schuhmann, J. Yao, G. Hong, T. M. Fu, C. M. Lieber, *Nano Lett.* **2017**, *17*, 5836.
[119] C. Xie, J. Liu, T.-M. Fu, X. Dai, W. Zhou, C. M. Lieber, *Nat. Mater.* **2015**, *14*, 1286.
[120] G. Hong, T. M. Fu, T. Zhou, T. G. Schuhmann, J. Huang, C. M. Lieber, *Nano Lett.* **2015**, *15*, 6979.
[121] X. Yang, T. Zhou, T. J. Zwang, G. Hong, Y. Zhao, R. D. Viveros, T. Fu, T. Gao, C. M. Lieber, *Nat. Mater.* **2019**, *18*, 510.
[122] M. E. Spira, A. Hai, *Nat. Nanotechnol.* **2013**, *8*, 83.
[123] A. Verkhratsky, O. A. Krishtal, O. H. Petersen, *Pflugers Arch. Eur. J. Physiol.* **2006**, *453*, 233.
[124] J. T. Robinson, M. Jorgolli, A. K. Shalek, M. H. Yoon, R. S. Gertner, H. Park, *Nat. Nanotechnol.* **2012**, *7*, 180.
[125] X. Duan, R. Gao, P. Xie, T. Cohen-Karni, Q. Qing, H. S. Choe, B. Tian, X. Jiang, C. M. Lieber, *Nat. Nanotechnol.* **2012**, *7*, 174.
[126] B. X. E. Desbiolles, E. De Coulon, A. Bertsch, S. Rohr, P. Renaud, *Nano Lett.* **2019**, *19*, 6173.
[127] A. Hai, J. Shappir, M. E. Spira, *J. Neurophysiol.* **2010**, *104*, 559.
[128] C. Xie, Z. Lin, L. Hanson, Y. Cui, B. Cui, *Nat. Nanotechnol.* **2012**, *7*, 185.
[129] M. Dipalo, G. Melle, L. Lovato, A. Jacassi, F. Santoro, V. Caprettini, A. Schirato, A. Alabastri, D. Garoli, G. Bruno, F. Tantussi, F. De Angelis, *Nat. Nanotechnol.* **2018**, *13*, 965.
[130] J. Abbott, T. Ye, L. Qin, M. Jorgolli, R. S. Gertner, D. Ham, H. Park, *Nat. Nanotechnol.* **2017**, *12*, 460.
[131] F. Santoro, J. Schnitker, G. Panaitov, A. Offenhäusser, *Nano Lett.* **2013**, *13*, 5379.
[132] J. F. Zimmerman, G. F. Murray, Y. Wang, J. M. Jumper, J. R. Austin, B. Tian, *Nano Lett.* **2015**, *15*, 5492.
[133] R. Parameswaran, J. L. Carvalho-De-Souza, Y. Jiang, M. J. Burke, J. F. Zimmerman, K. Koehler, A. W. Phillips, J. Yi, E. J. Adams, F. Bezanilla, B. Tian, *Nat. Nanotechnol.* **2018**, *13*, 260.
[134] Y. Zhao, J. Yao, L. Xu, M. N. Mankin, Y. Zhu, H. Wu, L. Mai, Q. Zhang, C. M. Lieber, *Nano Lett.* **2016**, *16*, 2644.
[135] Y. Zhao, S. S. You, A. Zhang, J. H. Lee, J. Huang, C. M. Lieber, *Nat. Nanotechnol.* **2019**, *14*, 783.
[136] A. Khademhosseini, R. Langer, *Nat. Protoc.* **2016**, *11*, 1775.
[137] X. Dai, W. Zhou, T. Gao, J. Liu, C. M. Lieber, *Nat. Nanotechnol.* **2016**, *11*, 776.
[138] I. R. Efimov, V. P. Nikolski, G. Salama, *Circ. Res.* **2004**, *95*, 21.
[139] R. Feiner, L. Engel, S. Fleischer, M. Malki, I. Gal, A. Shapira, Y. Shacham-Diamand, T. Dvir, *Nat. Mater.* **2016**, *15*, 679.
[140] S. Lee, D. Sasaki, D. Kim, M. Mori, T. Yokota, H. Lee, S. Park, K. Fukuda, M. Sekino, K. Matsuura, T. Shimizu, T. Someya, *Nat. Nanotechnol.* **2019**, *14*, 156.
[141] J. Rogers, Y. Huang, O. G. Schmidt, D. H. Gracias, *MRS Bull.* **2016**, *41*, 123.

[142] X. Wang, R. Feiner, H. Luan, Q. Zhang, S. Zhao, Y. Zhang, M. Han, Y. Li, R. Sun, H. Wang, T. L. Liu, X. Guo, H. Oved, N. Noor, A. Shapira, Y. Zhang, Y. Huang, T. Dvir, J. A. Rogers, *Extrem. Mech. Lett.* **2020**, *35*, 100634.
[143] Z. Yan, M. Han, Y. Shi, A. Badea, Y. Yang, A. Kulkarni, E. Hanson, M. E. Kandel, X. Wen, F. Zhang, Y. Luo, Q. Lin, H. Zhang, X. Guo, Y. Huang, K. Nan, S. Jia, A. W. Oraham, M. B. Mevis, J. Lim, X. Guo, M. Gao, W. Ryu, K. J. Yu, B. G. Nicolau, A. Petronico, S. S. Rubakhin, J. Lou, P. M. Ajayan, K. Thornton, G. Popescu, D. Fang, J. V. Sweedler, P. V. Braun, H. Zhang, R. G. Nuzzo, Y. Huang, Y. Zhang, J. A. Rogers, *Proc. Natl. Acad. Sci. U. S. A.* **2017**, *114*, E9455.
[144] Q. Li, K. Nan, P. Le Floch, Z. Lin, H. Sheng, T. S. Blum, J. Liu, *Nano Lett.* **2019**, *19*, 5781.
[145] M. S. Mannoor, Z. Jiang, T. James, Y. L. Kong, K. A. Malatesta, W. O. Soboyejo, N. Verma, D. H. Gracias, M. C. McAlpine, *Nano Lett.* **2013**, *13*, 2634.
[146] K. Qiu, Z. Zhao, G. Haghiashtiani, S.-Z. Guo, M. He, R. Su, Z. Zhu, D. B. Bhuiyan, P. Murugan, F. Meng, S. H. Park, C.-C. Chu, B. M. Ogle, D. A. Saltzman, B. R. Konety, R. M. Sweet, M. C. McAlpine, *Adv. Mater. Technol.* **2018**, *3*, 1700235.
[147] Y. A. Jodat, K. Kiaee, D. Vela Jarquin, R. L. De la Garza Hernández, T. Wang, S. Joshi, Z. Rezaei, B. A. G. de Melo, D. Ge, M. S. Mannoor, S. R. Shin, *Adv. Sci.* **2020**, *7*, 1901878.
[148] J. Abbott, T. Ye, K. Krenek, R. S. Gertner, S. Ban, Y. Kim, L. Qin, W. Wu, H. Park, D. Ham, *Nat. Biomed. Eng.* **2020**, *4*, 232.
[149] B. Shi, Z. Li, Y. Fan, *Adv. Mater.* **2018**, *30*, 1801511.
[150] Z. Xie, R. Avila, Y. Huang, J. A. Rogers, *Adv. Mater.* **2020**, *32*, 1902767.
[151] S. Sundaram, P. Kellnhofer, Y. Li, J. Y. Zhu, A. Torralba, W. Matusik, *Nature* **2019**, *569*, 698.
[152] Y. Huang, H. Wu, L. Xiao, Y. Duan, H. Zhu, J. Bian, D. Ye, Z. Yin, *Mater. Horizons* **2019**, *6*, 642.
[153] K. Sim, S. Chen, Z. Li, Z. Rao, J. Liu, Y. Lu, S. Jang, F. Ershad, J. Chen, J. Xiao, C. Yu, *Nat. Electron.* **2019**, *2*, 471.
[154] A. Sydney Gladman, E. A. Matsumoto, R. G. Nuzzo, L. Mahadevan, J. A. Lewis, *Nat. Mater.* **2016**, *15*, 413.

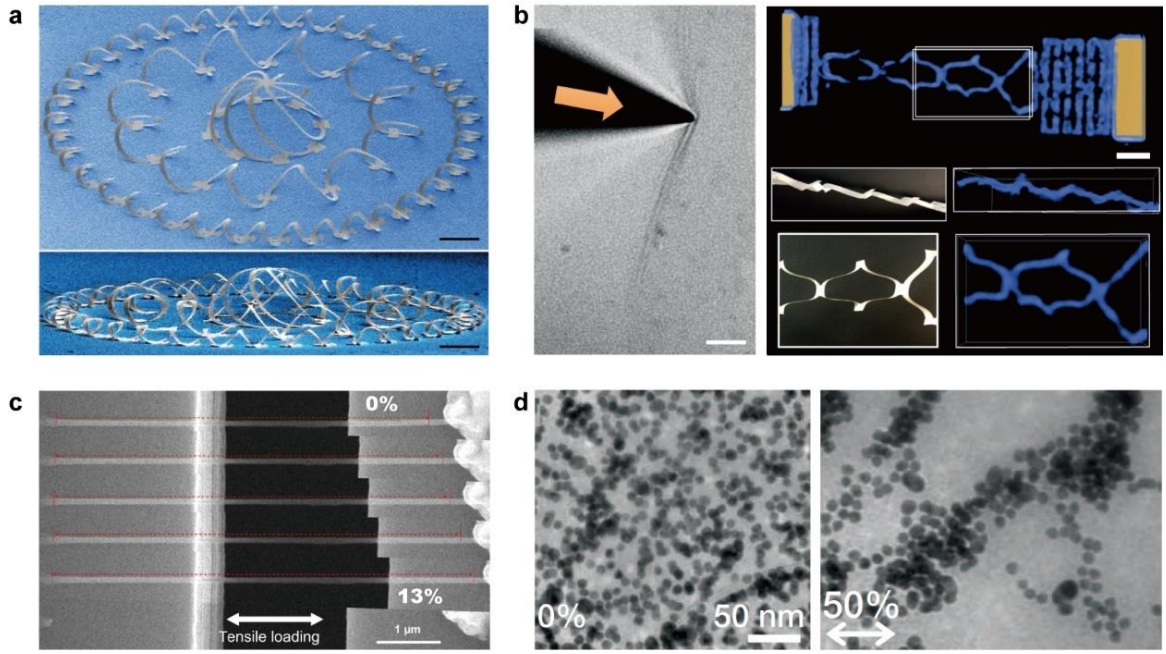

Figure 1. Inorganic nanomaterials for soft bioelectronics. (**a**) Complex 3D structures formed from controlled buckling of Si membranes with serpentine patterns, selectively bonded to a biaxially stretched elastomer substrate. Scale bars: 400 mm. Reproduced with permission.[8] Copyright 2015, American Association for the Advancement of Science. (**b**) Reconfigurable graphene structures. Left: folding and crumpling of a large graphene sheet induced by a micromanipulator. Right: 3D deformation of kirigami-patterned graphene sheet and its comparison with a paper model. Scale bars: 10 μm. Reproduced with permission.[15] Copyright 2015, Springer Nature. (**c**) Elongation of a Si NW (diameter, ~86 nm) characterized in-situ with SEM. Reproduced with permission.[25] Copyright 2016, American Association for the Advancement of Science. (**d**) Transmission electron microscopy (TEM) images of Au NPs dispersed in elastomer matrix, showing that the Au NPs self-organize into chains upon stretching. Reproduced with permission.[26] Copyright 2013, Springer Nature.

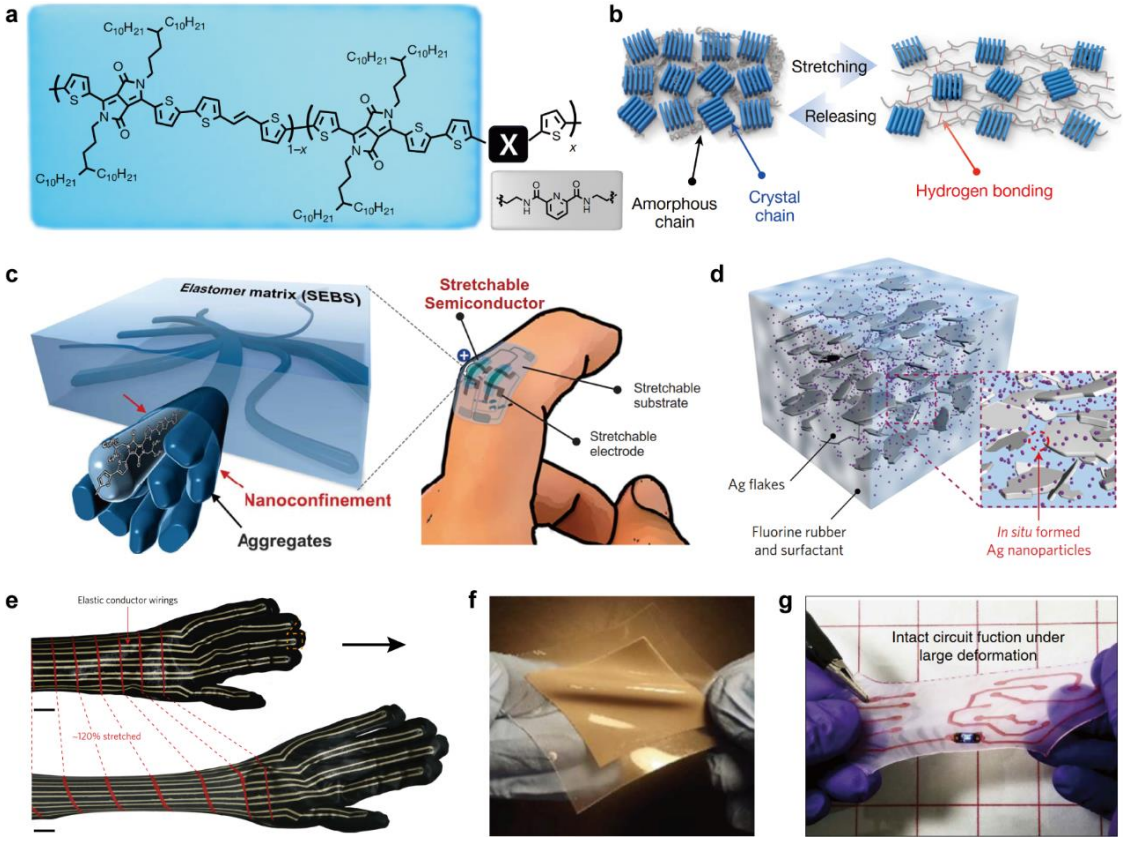

Figure 2. Polymeric and composite materials for soft bioelectronics. (**a**) Chemical structure of a stretchable and healable semiconducting polymer. The "X" denotes non-conjugated, hydrogen-bond-forming moieties inserted into the DPP-based backbone, as exemplified by 2,6-pyridine dicarboxamide (PDCA). (**b**) Schematic illustration of the stretching-induced structural reconfiguration of the polymer shown in (**a**). Reproduced with permission.[36] Copyright 2016, Springer Nature. (**c**) A schematic of the percolating network consisting of semiconducting polymer nanofibrils formed in the elastomer matrix, which could be used for building stretchable and wearable transistors. Reproduced with permission.[37] Copyright 2017, American Association for the Advancement of Science. (**d**) A schematic illustration of printable elastic conductor involving Ag NPs formed in-situ in the elastomer matrix, derived from the dispersed, micrometer-sized Ag flakes. (**e**) Photographs of stretchable and fully printed sensor networks based on the composites shown in (**d**). Scale bar: 2 cm. Reproduced with permission.[46] Copyright 2017, Springer Nature. (**f**) A photograph of Galinstan dispersed in silicone elastomer matrix. Reproduced with permission.[50] Copyright 2015, Wiley-VCH. (**g**) A photograph of stretchable electrical circuit based on ionically conductive hydrogels embedded in silicone elastomer matrix. Reproduced with permission.[59] Copyright 2016, Springer Nature.

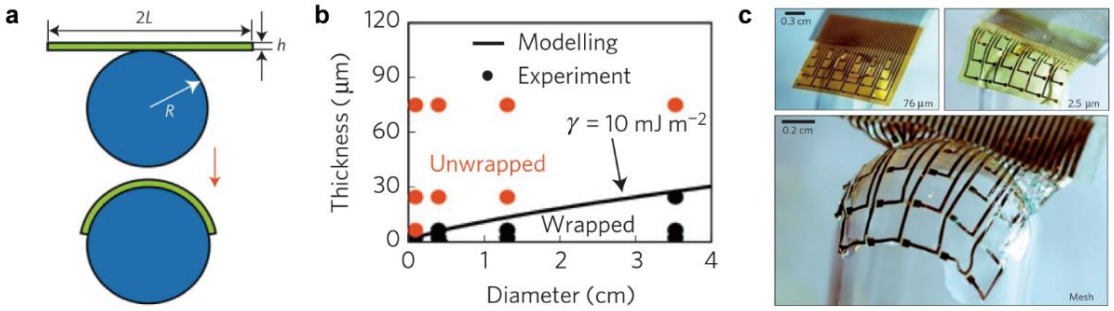

Figure 3. Mechanics of conformal devices. (**a**) A model involving a polyimide sheet to be wrapped on a cylindrical surface. (**b**) The state of wrapping as a function of the thickness of the device and the radius of the cylinder shown in (**a**). (**c**) Images of representative devices placed on a glass hemisphere, showing the effects of the device thickness and the mesh design. Reproduced with permission.[60] Copyright 2010, Springer Nature.

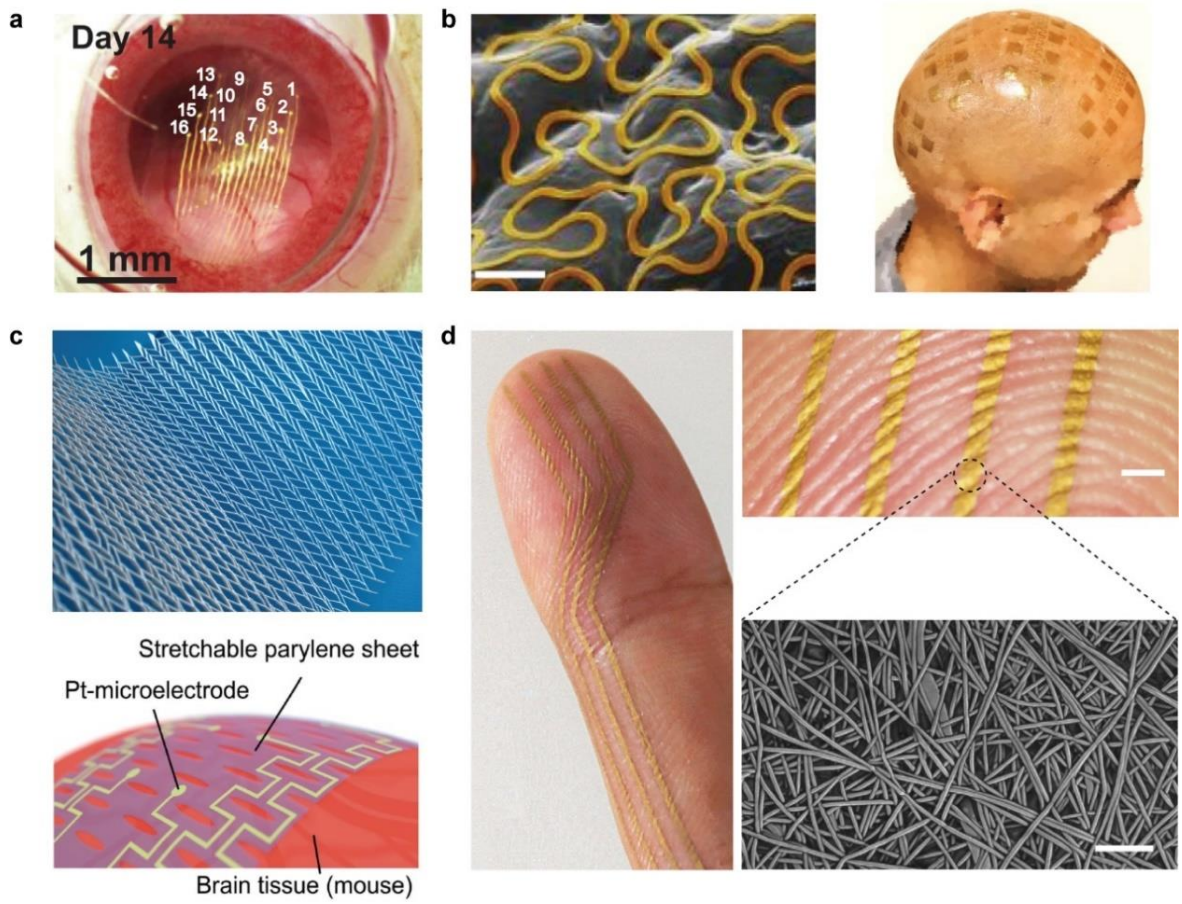

Figure 4. Meshes and kirigami devices for organ-conformal integration. (**a**) Mesh electrodes integrated on the retina of a living mouse after 14 days of implantation. Reproduced with permission.[61] Copyright 2018, American Association for the Advancement of Science. (**b**) Left: A SEM image of fractal serpentines laminated on a skin replica. Scale bar: 500 μm. Reproduced with permission.[65] Copyright 2014, Springer Nature. Right: An array of serpentine mesh electrodes integrated over the full scalp of a patient. Reproduced with permission.[70] Copyright 2019, Springer Nature. (**c**) Top: A photograph of a representative kirigami structure. Reproduced with permission.[72] Copyright 2015, Springer Nature. Bottom: A schematic of kirigami-patterned electrodes array integrated on the surface of mouse brain. Reproduced with permission.[76] Copyright 2018, Wiley-VCH. (**d**) Electrodes based on gold nanomeshes integrated on the fingertip. Scale bars: top: 1 mm, bottom: 5 μm. Reproduced with permission.[77] Copyright 2017, Springer Nature.

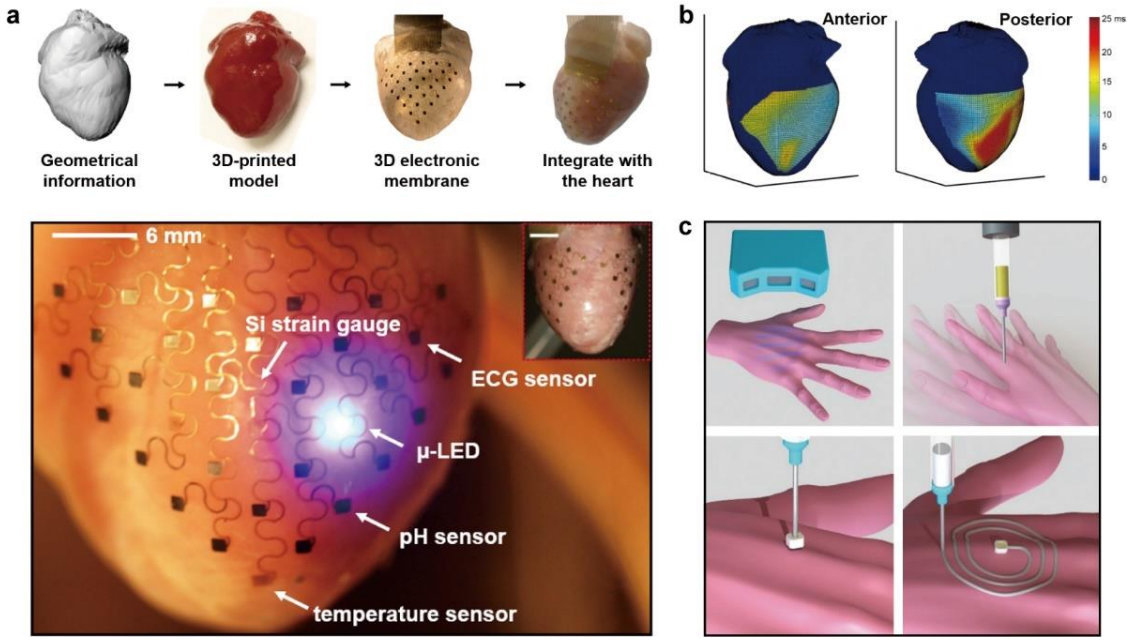

Figure 5. Design and fabrication of organ-specific electronics. (**a**) Top: The fabrication process for a heart-specific electronic membrane. Bottom: Photographs of 3D electronic membranes integrated across the entire surface of a rabbit heart. (**b**) Activation mapping of a Langendorff-perfused rabbit heart from both anterior and posterior surfaces, measured with a 3D electronic membrane. Reproduced with permission.[79] Copyright 2014, Springer Nature. (**c**) Schematics of a close-loop system for custom fabrication of skin-conformal electronics. It involves 3D imaging, motion tracking and 3D printing of functional components. Reproduced with permission.[86] Copyright 2018, Wiley-VCH.

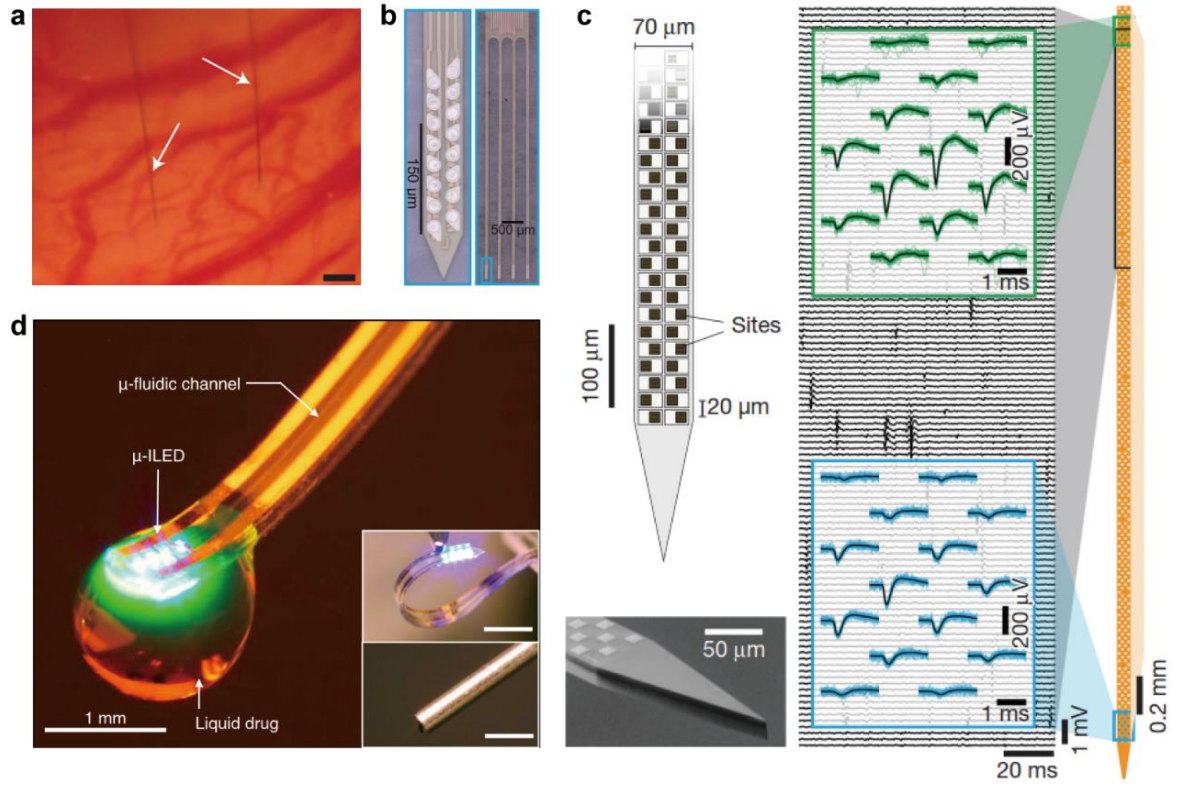

Figure 6. Miniaturized neural probes. (**a**) Composite microwire electrodes implanted into the cortex of a rat. Scale bar: 100 µm. Reproduced with permission.[93] Copyright 2012, Springer Nature. (**b**) An array of polymer-based, Michigan-type probes involving 64 electrodes. Such array could be deployed in groups allowing for up to 1024 electrodes implanted in a rat brain. Reproduced with permission.[102] Copyright 2019, Elsevier Inc. (**c**) A CMOS-based Si probe involving 960 neural electrodes. The insets show neural activities recorded on day 58 after implantation. Reproduced with permission.[101] Copyright 2017, Springer Nature. (**d**) An optofluidic neural probe for programed in-vivo pharmacology and optogenetics. The insets show a comparison of a representative device (top) with a conventional metal cannula (bottom). Scale bars, 1 mm. Reproduced with permission.[109] Copyright 2015, Elsevier Inc.

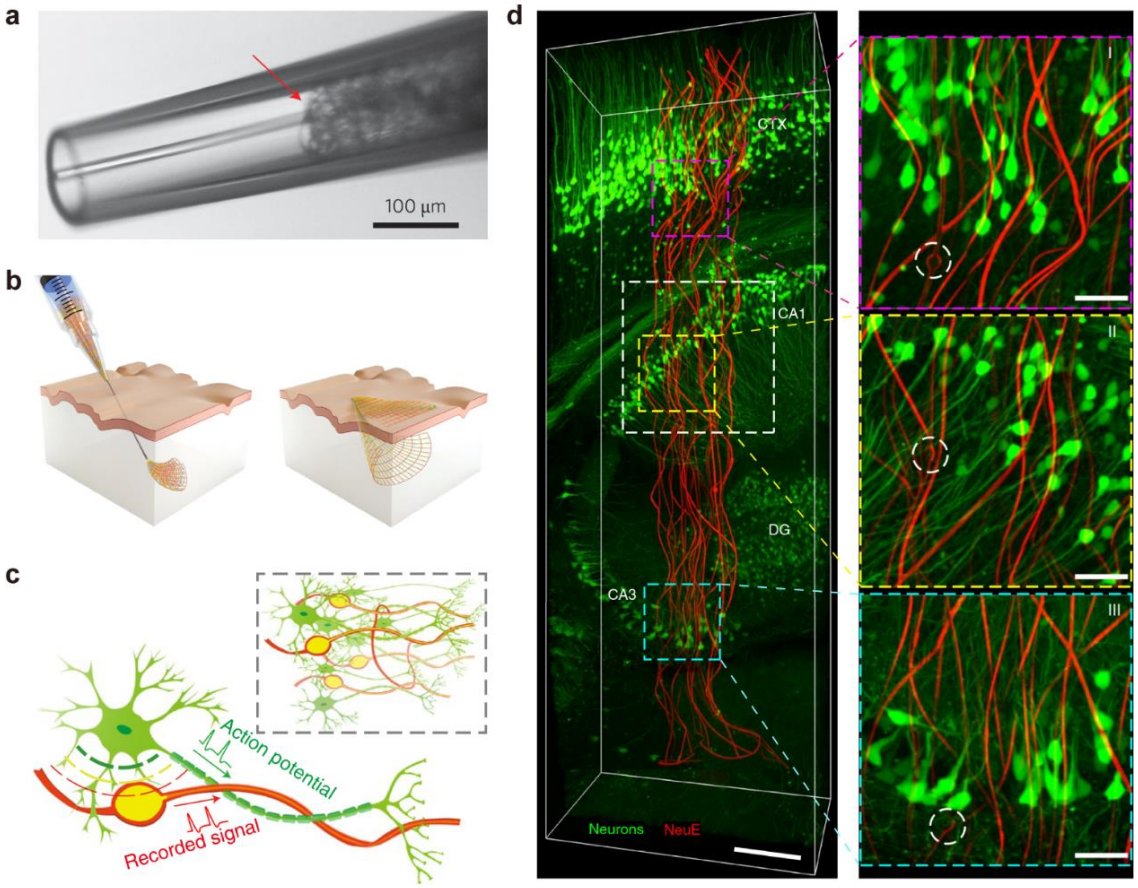

Figure 7. Injectable mesh devices for interpenetrating neuro-electronic interfaces. (**a**) An optical image of mesh electronics fitted into a glass needle (inner diameter 95 µm) and ready for injection. (**b**) Schematics of the injection process for a mesh probe. Reproduced with permission.[115] Copyright 2015, Springer Nature. (**c**) Schematics of NeuE interfacing with natural neurons, showing their structural similarity at subcellular levels. Neurons: green; electrodes and interconnects: yellow; polymer layers: red. (**d**) 3D reconstructed fluorescent images showing the interpenetrating interface between neurons (green) and NeuE (red) at 6 weeks post-implantation. The electrodes are highlighted with white dashed circles. Scale bars: left: 200 µm, right: 50 µm. Reproduced with permission.[121] Copyright 2019, Springer Nature.

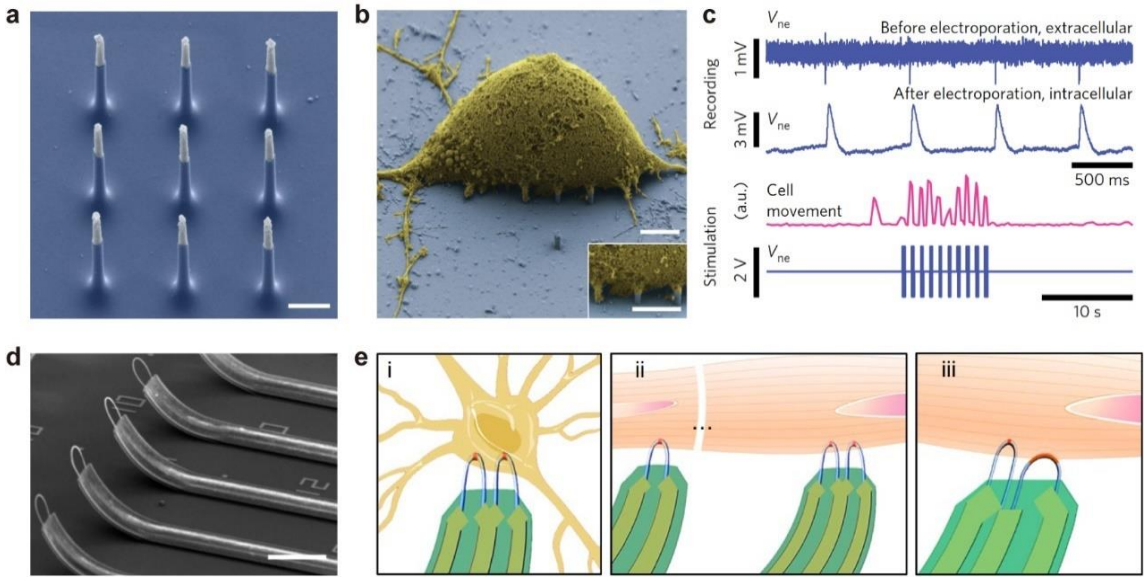

Figure 8. 3D nanoelectronics for intracellular recordings. (**a**) An SEM image of vertical nanoelectrodes based on Si. False coloring shows metal-coated tips. Scale bar: 1 µm. (**b**) A SEM image of a rat cortical cell on top of vertical nanoelectrodes. The inset shows the membrane-electrode junction. Scale bars: 2.5 µm. Reproduced with permission.[124] Copyright 2012, Springer Nature. (**c**) Top: comparison of extracellular and intracellular signals from a cardiomyocyte, measured by an array of vertical nanoelectrodes. Bottom: stimulation of a cardiomyocyte using vertical nanoelectrodes, with synchronized cell movement analyzed from video differentials. Reproduced with permission.[130] Copyright 2017, Springer Nature. (**d**) A SEM image of an array of U-shaped NW-FET probes. Scale bar: 10 µm. Reproduced with permission.[134] Copyright 2016, American Chemical Society. (**e**) Schematics of simultaneous multisite intracellular recording using scalable NW-FET probes. (i) multisite intracellular recording from a single cell; (ii) multiplexed intracellular recording from different cells; (iii) simultaneous intracellular/extracellular recording from one cell. Reproduced with permission.[135] Copyright 2019, Springer Nature.

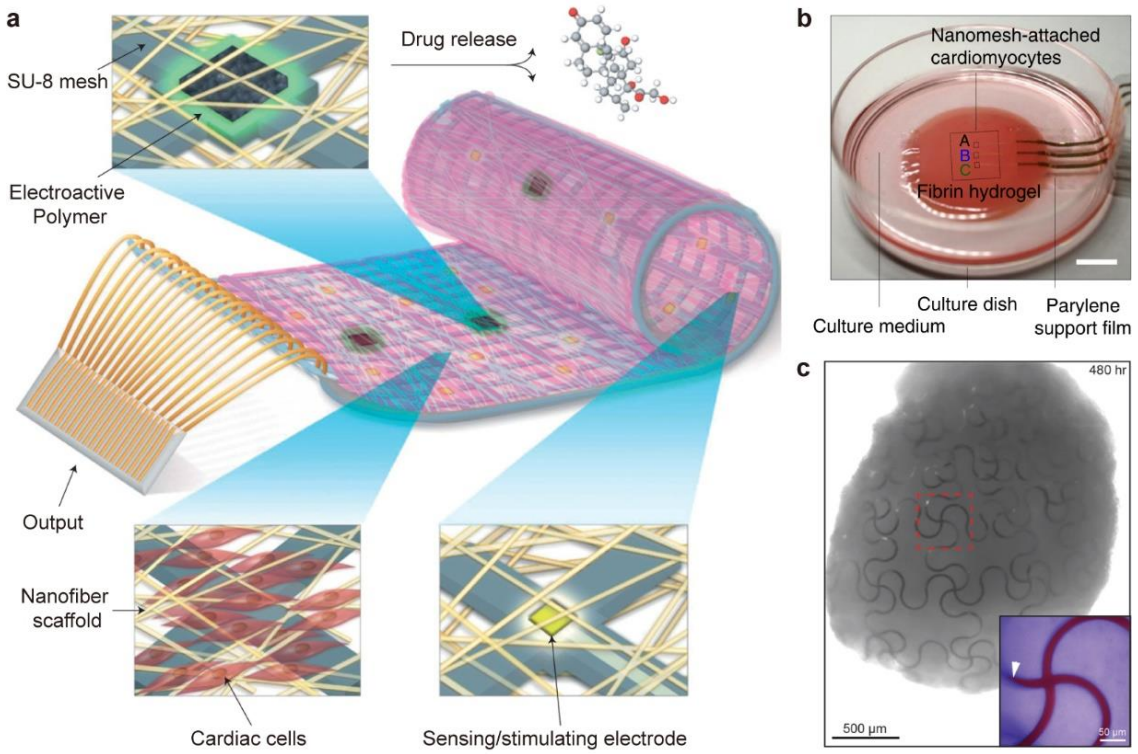

Figure 9. Electronic scaffolds for synthetic tissues. (**a**) Schematics of a multifunctional electronic mesh capable of cell attachment, in-situ sensing/stimulation, and controlled release of drugs. Reproduced with permission.[139] Copyright 2016, Springer Nature. (**b**) A photograph of a cardiomyocyte cell culture with embedded nano-mesh electronics. Scale bar: 1 cm. Reproduced with permission.[140] Copyright 2018, Springer Nature. (**c**) An optical image of an electronics-integrated cardiac organoid. The inset shows a magnified view of the stretchable electronic mesh. Reproduced with permission.[144] Copyright 2019, American Chemical Society.

YongAn Huang received a B.S. degree (2001), M.S. degree (2004), and Ph.D. degree (2007) from the Northwestern Polytechnical University, Xian, China. Since 2007, he has been a Faculty member at the State Key Laboratory of Digital Manufacturing Equipment and Technology, Huazhong University of Science and Technology (HUST), where he became a professor in 2014. His research interests include flexible electronics manufacturing and advanced printing.

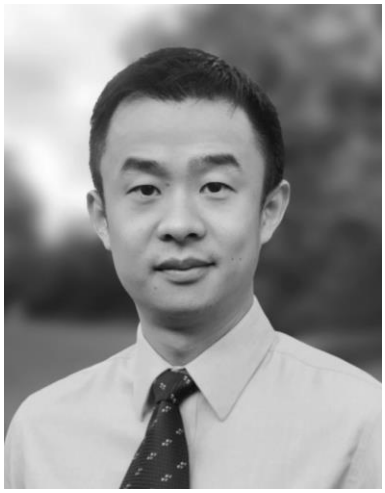

Lizhi Xu is an Assistant Professor at the Department of Mechanical Engineering, The University of Hong Kong. He obtained his B.S. degree (2009) in Applied Physics from Beihang University, and his Ph.D. degree (2014) in Materials Science and Engineering from University of Illinois, Urbana-Champaign. He worked as a Postdoctoral Research Fellow at the University of Michigan from 2015-2018 before joining the University of Hong Kong. His research interests involve biomimetic materials, soft electronics, biomedical devices and micro-/nanofabrication.

ToC Entry: Soft electronics enable biocompatible interfaces for physiological sensing and stimulation. However, their typical forms as 2D sheets create difficulties for integration with organs and tissues with complex 3D geometry. Recent strategies involve a transformation of soft electronic tools for building adaptive 3D interfaces with natural organs and tissues, providing advanced capabilities for biological research and therapeutic innovation.

Keyword: soft electronics, 3D bioelectronics, biomedical devices, biointerfaces, physiological sensing and stimulation

Hegeng Li, Hongzhen Liu, Mingze Sun, YongAn Huang* and Lizhi Xu*

Title: 3D Interfacing Between Soft Electronic Tools and Complex Biological Tissues

ToC figure